

DENSITY ESTIMATION VIA PERIODIC SCALED KOROBOV KERNEL METHOD WITH EXPONENTIAL DECAY CONDITION*

ZIYANG YE[†], HAOYUAN TAN[‡], XIAOQUN WANG[†], AND ZHIJIAN HE[§]

Abstract. We propose the periodic scaled Korobov kernel (PSKK) method for nonparametric density estimation on \mathbb{R}^d . By first wrapping the target density into a periodic version through modulo operation and subsequently applying kernel ridge regression in scaled Korobov spaces, we extend the kernel approach proposed by Kazashi and Nobile (SIAM J. Numer. Anal., 2023) and eliminate its requirement for inherent periodicity of the density function. This key modification enables effective estimation of densities defined on unbounded domains. We establish rigorous mean integrated squared error (MISE) bounds, proving that for densities with smoothness of order α and exponential decay, our method achieves the $\mathcal{O}(M^{-1/(1+1/(2\alpha)+\epsilon)})$ MISE convergence rate with an arbitrarily small $\epsilon > 0$. While matching the convergence rate of the previous kernel approach, our approach applies to a broader class of non-periodic distributions. Numerical experiments confirm the theoretical results and demonstrate significant improvement over traditional kernel density estimation in large-sample regimes.

Key words. density estimation, periodization, kernel method, scaled Korobov space

MSC codes. 62G07, 65D40

1. Introduction. Density estimation is a fundamental challenge in statistics with broad applications in uncertainty quantification [11, 24, 25, 30, 31], machine learning [3, 36, 39, 41], and data analysis [2, 13, 15, 34]. Unlike parametric methods [38], which assume a specific form for the distribution (e.g., Gaussian), the density estimation in which we are interested are often non-parametric or semi-parametric, allowing them to adapt to the complexity of the data without strong assumptions about the distribution. Classical methods, such as kernel density estimation (KDE), are effective in low dimensions but may suffer from the curse of dimensionality [6]. Generally speaking, it is difficult to solve density estimation problems exceeding 6 dimensions using KDE methods. Additionally, traditional methods often perform poorly when the density function is multi-modal [34].

With these challenges in mind, in this paper we consider the density estimation problem over \mathbb{R}^d . Let $(\Omega, \mathcal{F}, \mathbb{P})$ be a probability space and $(\mathbb{R}^d, \mathcal{B}(\mathbb{R}^d))$ be a measurable space, where $\mathcal{B}(\mathbb{R}^d)$ denotes the Borel sets in \mathbb{R}^d . Given M independent random vectors $Y_1, \dots, Y_M : \Omega \rightarrow \mathbb{R}^d$ that follow an identical distribution defined by a density f with respect to the Lebesgue measure on \mathbb{R}^d , we aim to obtain an estimator \bar{f} so that the mean integrated squared error (MISE), defined as

$$\mathbb{E} \left[\int_{\mathbb{R}^d} |\bar{f}(\mathbf{x}) - f(\mathbf{x})|^2 d\mathbf{x} \right],$$

is small. For this error, traditional methods like KDE can only achieve a convergence

*Submitted to the editors DATE.

Funding: The work of the first and third authors was funded by the National Science Foundation of China (grant 72071119). The work of the fourth authors was funded by the Guangdong Basic and Applied Basic Research Foundation (grant 2025A1515011888 and 2024A1515011876).

[†]Department of Mathematical Sciences, Tsinghua University, Beijing 100084, People's Republic of China (zy23@mails.tsinghua.edu.cn, wangxiaoqun@mail.tsinghua.edu.cn).

[‡]School of Mathematics, South China University of Technology, Guangzhou 510641, People's Republic of China (202410188273@mail.scut.edu.cn).

[§]Corresponding author. School of Mathematics, South China University of Technology, Guangzhou 510641, People's Republic of China (hezhijian@scut.edu.cn).

rate of $\mathcal{O}(M^{-\frac{4}{d+4}})$, which degrades exponentially as the dimension d increases [34]. Beyond this traditional approach, numerous alternative density estimation methods have emerged, such as the maximum a posteriori (MAP) estimator [14, 40], techniques based on minimizing Fisher divergence [35], supervised deep learning approaches [4], and deep generative neural networks [23]. While these methods offer advantages in overcoming scalability or adaptability limitations associated with KDE, a quantitative analysis of their MISE convergence rates in general dimensions remains largely lacking.

In order to obtain a higher MISE convergence rate, a regularized least squares approach is considered in many works [16, 20, 29, 32]. This approach supposes that the density function f lies in some inner product space W and want to compute finite-sample approximations of f by discretizing the minimization problem

$$(1.1) \quad \min_{g \in V} \|f - g\|_{L^2(\mathbb{R}^d)}^2 + \lambda \|g\|_W^2,$$

where V is a finite dimensional subspace of W , $\lambda > 0$ is a regularization parameter, and $\|\cdot\|_W$ denotes the norm induced by the inner product $\langle \cdot, \cdot \rangle_W$ on W . The discretized minimization problem (1.1) is equivalent to find $g \in V$ such that

$$(1.2) \quad \langle g, v \rangle_{L^2(\mathbb{R}^d)} + \lambda \langle g, v \rangle_W = \frac{1}{M} \sum_{m=1}^M v(Y_m), \quad \text{for all } v \in V.$$

The approximation of type (1.2) is a variant of what Hegland et al. proposed in [16], in which V was considered to be a standard finite element space. However, the approximation in V becomes infeasible when the dimension d is large. Peherstorfer et al. [29] considered V to be the span of sparse-grid basis functions, but the density functions they considered are actually defined on a bounded domain, and the MISE error bound is not investigated. Roberts and Bolt [32] proposed a method similar to that in [29], but omitted the regularization term. Their estimator has an MISE bound of $\mathcal{O}(|\log M|^{2d} M^{-\frac{4}{d}})$ with an implied constant exponentially increasing in d . Their conclusions are only applicable to density functions defined on the unit cube, and their MISE convergence rate still has a gap to the optimal lower bound in [5], which is $\mathcal{O}(M^{-1})$.

More recently, Kazashi and Nobile [20] applied the approximation (1.2) to density functions in the reproducing kernel Hilbert space (RKHS). This approach is widely used in density ratio estimation [18, 19, 37, 42] but remains relatively rare for obtaining estimators and analyzing MISE in density estimation problems. In Kazashi and Nobile's setting the function space W is an RKHS with a reproducing kernel $K : D \times D \rightarrow \mathbb{R}$, where D is a region in \mathbb{R}^d , and the finite-dimensional subspace V is chosen to be

$$(1.3) \quad V = V(X) = \text{span}\{K(x_k, \cdot) | k = 1, \dots, N\},$$

where $X = \{\mathbf{x}_1, \dots, \mathbf{x}_N\} \subset D$ is a preselected point set. They developed a theoretical framework for analyzing MISE for a general reproducing kernel K that admits an L^2 orthonormal expansion. In particular, for the density function f in the weighted Korobov space over $[0, 1]^d$, they proved that the total MISE is $\mathcal{O}(M^{-1/(1+1/(2\alpha)+\epsilon)})$, where 2α is the smoothness parameter of the Korobov space and $\epsilon > 0$ is an arbitrary positive number. However, the assumption that f lies in the weighted Korobov space forces the density function f to be a periodic function on $[0, 1]^d$, which limits the applicability of the error bound.

To overcome the limitations associated with periodicity and compact support of the density functions discussed in [20], we propose the periodic scaled Korobov kernel (PSKK) method. Specifically, we set $K = K_{\alpha,a,d} : [-a, a]^d \rightarrow \mathbb{R}$ to be the kernel of the scaled Korobov space over $[-a, a]^d$ with even smoothness parameter 2α (see [27] for detail) in the density estimation framework in [20] and establish the MISE bound with the scaling parameter a . In order to handle the periodicity that Korobov spaces need, we artificially map the random vector to $[-a, a]^d$ via modulo $2a$ operation. More specifically, for each $1 \leq m \leq M$, we transform the random vector $Y_m = (Y_{m,1}, \dots, Y_{m,d})^\top$ into $\tilde{Y}_m = (\tilde{Y}_{m,1}, \dots, \tilde{Y}_{m,d})^\top$ by defining

$$\tilde{Y}_{m,j} = (Y_{m,j} \bmod 2a) - a \in [-a, a),$$

for all $1 \leq j \leq d$. Then $\tilde{Y}_1, \dots, \tilde{Y}_M$ are iid random vectors with periodic density function

$$(1.4) \quad \tilde{f}(\mathbf{x}) = \sum_{\mathbf{k} \in \mathbb{Z}^d} f(\mathbf{x} + 2a\mathbf{k}), \quad \forall \mathbf{x} \in [-a, a]^d,$$

where \mathbb{Z} denotes the set of integers.

Notably, the periodic density function \tilde{f} can be interpreted as the wrapped version of f , a concept frequently employed in toroidal density estimation (see references [1, 9, 26]). Unlike existing approaches that directly estimate the wrapped density function on a predefined torus, our method proposes to first transform the original density f into its wrapped version \tilde{f} and then perform the density estimation on \tilde{f} . By allowing the scaling parameter a to grow with M , we ensure that \tilde{f} converges to f with increasing accuracy. Specifically, if f satisfies the exponential decay condition up to order α (Definition 4.1), we prove that the discrepancy between \tilde{f} and f decays exponentially with a . Based on this result we apply the approximation (1.2) to \tilde{f} as follows: find $\tilde{f}_{\tilde{\mathbf{Y}}}^\lambda \in V_N$ such that

$$\left\langle \tilde{f}_{\tilde{\mathbf{Y}}}^\lambda, v \right\rangle_{L^2([-a, a]^d)} + \lambda \left\langle \tilde{f}_{\tilde{\mathbf{Y}}}^\lambda, v \right\rangle_{K_{\alpha,a,d}} = \frac{1}{M} \sum_{m=1}^M v(\tilde{Y}_m), \quad \text{for all } v \in V_N,$$

where $\langle \cdot, \cdot \rangle_{K_{\alpha,a,d}}$ denotes the inner product in the scaled Korobov space over $[-a, a]^d$, $\tilde{\mathbf{Y}} := \{\tilde{Y}_1, \dots, \tilde{Y}_M\}$, $\lambda > 0$ is a ‘‘regularization’’ parameter, and

$$V_N := V_N(X) := \text{span}\{K_{\alpha,a,d}(\mathbf{x}_k, \cdot) | k = 1, \dots, N\},$$

with a preselected point set $X = \{\mathbf{x}_1, \dots, \mathbf{x}_N\} \subset [-a, a]^d$. We then define the PSKK estimator

$$\bar{f}(\mathbf{x}) = f_{\tilde{\mathbf{Y}}}^\lambda(\mathbf{x}) := \begin{cases} \max\{\tilde{f}_{\tilde{\mathbf{Y}}}^\lambda(\mathbf{x}), 0\}, & \text{for } \mathbf{x} \in [-a, a]^d, \\ 0, & \text{for } \mathbf{x} \in \mathbb{R}^d \setminus [-a, a]^d, \end{cases}$$

based on the sample set $\mathbf{Y} := \{Y_1, \dots, Y_M\}$ and establish that with appropriate choices of a, N and λ , the MISE of the PSKK estimator achieves $\mathcal{O}(M^{-1/(1+1/(2\alpha)+\epsilon)})$ convergence rate. Remarkably, although the constant in our MISE bound depends on the dimension d , the MISE bound can asymptotically tend to $\mathcal{O}(M^{-1})$ provided that f is infinitely differentiable over \mathbb{R}^d .

The structure of this paper is organized as follows. Section 2 reviews fundamental concepts related to both the standard and scaled Korobov spaces, as well as providing

a detailed revisit of Kazashi and Nobile's estimator in [20]. Section 3 focuses on density functions in the scaled Korobov spaces and obtains the MISE bound with the scaled parameter a . In Section 4, we apply the density estimation to the wrapped version of the target density function f and obtain the total MISE bound under the exponential decay assumption. Section 5 discusses some details in implementing our PSKK method. Section 6 provides a portion of numerical experiments to support the theoretical results, while the other portion is presented in the appendix. Finally, in Section 7, we draw the conclusions of the paper.

2. Notations and backgrounds. For a measurable space (D, \mathcal{B}, μ) , let $L^2_\mu(D)$ denote the space of square-integrable functions with respect to the measure μ over the domain D . Specifically, $L^2(D)$ refers to the case where μ is the Lebesgue measure. Denote $\mathcal{H}(K)$ as the RKHS with reproducing kernel $K : D \times D \rightarrow \mathbb{R}$, where D is a region in \mathbb{R}^d . Let $\|f\|_K$ and $\langle f, g \rangle_K$ be the corresponding norm of $f \in \mathcal{H}(K)$ and inner product of f and g for $f, g \in \mathcal{H}(K)$. By the reproducibility of $\mathcal{H}(K)$ we have

$$\langle f, K(\cdot, \mathbf{y}) \rangle_K = f(\mathbf{y}), \quad \forall \mathbf{y} \in D \text{ and } \forall f \in \mathcal{H}(K).$$

For any $\mathbf{a}, \mathbf{b} \in \mathbb{R}^d$ with $a_j \leq b_j$ for $j = 1, \dots, d$, let $[\mathbf{a}, \mathbf{b}] = \prod_{j=1}^d [a_j, b_j]$. For any $k, s \in \mathbb{Z}$ with $k \leq s$, let $\{k:s\} = \{k, k+1, \dots, s\}$. For any subset $u \subset \{1:d\}$, let $-u$ denote the complement of u , \mathbf{y}_u denote the vector $(y_j)_{j \in u}$, and let $[\mathbf{a}_u, \mathbf{b}_u] = \prod_{j \in u} [a_j, b_j]$. Additionally, we denote $\mathbf{1}$ as the d -dimensional all-ones vector.

To denote the partial derivatives of f , we adopt the following notations

$$f^{(\boldsymbol{\tau})}(\mathbf{x}) = \prod_{j=1}^d \frac{\partial^{\tau_j} f}{\partial x_j^{\tau_j}}(\mathbf{x}), \quad \partial_u^k f(\mathbf{x}) = \prod_{j \in u} \frac{\partial^k f}{\partial x_j^k}(\mathbf{x}), \quad \forall \boldsymbol{\tau} \in \mathbb{N}_0^d, k \in \mathbb{N}_0, u \subset \{1:d\},$$

where \mathbb{N}_0 denotes the set of non-negative integers.

We also introduce the periodicity on $[\mathbf{a}, \mathbf{b}]$.

DEFINITION 2.1. For a function $h : [\mathbf{a}, \mathbf{b}] \rightarrow \mathbb{R}$, we say h is periodic on $[\mathbf{a}, \mathbf{b}]$ if there exists a function $\bar{h} : \mathbb{T} \rightarrow \mathbb{R}$, where $\mathbb{T} = \{(\theta_1, \dots, \theta_d) : \theta_i \in [0, 2\pi), i = 1, \dots, d\}$ is a d -torus, such that

$$h(x_1, \dots, x_d) = \bar{h} \left(\frac{2\pi x_1}{b_1 - a_1} + 2k_1\pi, \dots, \frac{2\pi x_d}{b_d - a_d} + 2k_d\pi \right),$$

where $k_i \in \mathbb{Z}$ such that $\frac{2\pi x_i}{b_i - a_i} + 2k_i\pi \in [0, 2\pi)$, for $i = 1, \dots, d$. Furthermore, for $\alpha \in \mathbb{N}$, we say h is C^α -periodic on $[\mathbf{a}, \mathbf{b}]$ if $\bar{h}^{(\boldsymbol{\tau})}$ is continuous on \mathbb{T} for every $\boldsymbol{\tau} \in \{0:\alpha\}^d$.

2.1. Korobov space on the unit cube. This subsection focuses on periodic functions over the unit cube $[0, 1]^d$ admitting an absolutely convergent Fourier series representation

$$f(\mathbf{x}) = \sum_{\mathbf{h} \in \mathbb{Z}^d} \hat{f}(\mathbf{h}) \exp(2\pi i \langle \mathbf{h}, \mathbf{x} \rangle), \quad \hat{f}(\mathbf{h}) := \int_{[0,1]^d} f(\mathbf{x}) \exp(-2\pi i \langle \mathbf{h}, \mathbf{x} \rangle) d\mathbf{x},$$

where $\langle \cdot, \cdot \rangle$ denotes the Euclidean inner product on \mathbb{R}^d . The Korobov space is an RKHS defined as follows.

DEFINITION 2.2. For $\alpha \in \mathbb{N}$, the space $\mathcal{H}(K_{\alpha,d})$ is a Korobov space on the unit

cube $[0, 1]^d$, which is an RKHS with the inner product

$$\langle f, g \rangle_{K_{\alpha, d}} := \sum_{\mathbf{h} \in \mathbb{Z}^d} \widehat{f}(\mathbf{h}) \overline{\widehat{g}(\mathbf{h})} r_{\alpha, d}(\mathbf{h})^2,$$

and the reproducing kernel

$$K_{\alpha, d}(\mathbf{x}, \mathbf{y}) := \sum_{\mathbf{h} \in \mathbb{Z}^d} \frac{\exp(2\pi i \langle \mathbf{h}, (\mathbf{x} - \mathbf{y}) \rangle)}{r_{\alpha, d}(\mathbf{h})^2} = \prod_{j=1}^d \left(1 + (-1)^{\alpha+1} \frac{B_{2\alpha}(|x_j - y_j|)}{(2\alpha)!} \right),$$

where $B_k(x)$ is the Bernoulli polynomial of degree k and

$$r_{\alpha, d}(\mathbf{h}) = \prod_{j=1}^d r_{\alpha}(h_j), \quad r_{\alpha}(h_j) = \begin{cases} 1, & \text{for } h_j = 0, \\ |2\pi h_j|^{\alpha}, & \text{for } h_j \neq 0. \end{cases}$$

Remark 2.3. The Korobov space that we consider here is a special case of the Korobov spaces in [20] with even smoothness parameter 2α and product weights $\gamma_u = (2\pi)^{-\alpha|u|}$.

It should be noted that $\mathcal{H}(K_{\alpha, d})$ consists of all functions that are C^{α} -periodic on $[0, 1]^d$, and the inner product of Korobov space $\mathcal{H}(K_{\alpha, d})$ can be expressed in the following form

$$\langle f, g \rangle_{K_{\alpha, d}} = \sum_{u \subset \{1: d\}} \int_{[0, 1]^{|u|}} \left(\int_{[0, 1]^{d-|u|}} \partial_u^{\alpha} f(\mathbf{x}) d\mathbf{x}_{-u} \right) \left(\int_{[0, 1]^{d-|u|}} \partial_u^{\alpha} g(\mathbf{x}) d\mathbf{x}_{-u} \right) d\mathbf{x}_u.$$

2.2. Korobov space on a box. We now define the Korobov space on a box $[-a, a]^d \subset \mathbb{R}^d$ with $a > 0$. Firstly, we shall recall the ‘scaled’ version of trigonometric polynomials and Bernoulli polynomials (see [27] for details). For any $h \in \mathbb{Z}$, let

$$\varphi_{a, h}(x) = \frac{1}{\sqrt{2a}} \exp\left(2\pi i h \frac{x+a}{2a}\right).$$

For $\mathbf{h} \in \mathbb{Z}^d$, let $\varphi_{a, d, \mathbf{h}}(\mathbf{x}) = \prod_{j=1}^d \varphi_{a, h_j}(x_j)$. Then $\{\varphi_{a, d, \mathbf{h}}\}$ constitutes a standard orthonormal system in $L^2([-a, a]^d)$.

For any $k \in \mathbb{N}$, $x \in [-a, a]$, let

$$B_{a, k}(x) = (2a)^{k-1} B_k((x-a)/(2a)).$$

We also define the ‘scaled’ version of periodic Bernoulli polynomials as follows

$$\widetilde{B}_{a, k}(x) = B_{a, k}(x), \text{ for } x \in [-a, a],$$

and $\widetilde{B}_{a, k}(x) = \widetilde{B}_{a, k}(x + t(b-a))$ for any $t \in \mathbb{Z}$, $x \in \mathbb{R}$.

Now we consider the ‘periodic’ space on the box $[-a, a]^d$, in which the function has the following form of absolutely converging Fourier series with respect to $\varphi_{a, d, \mathbf{h}}$

$$f(\mathbf{x}) = \sum_{\mathbf{h} \in \mathbb{Z}^d} \widehat{f}_{a, d}(\mathbf{h}) \varphi_{a, d, \mathbf{h}}(\mathbf{x}), \quad \widehat{f}_{a, d}(\mathbf{h}) = \int_{[\mathbf{a}, \mathbf{b}]} f(\mathbf{x}) \overline{\varphi_{a, d, \mathbf{h}}(\mathbf{x})} d\mathbf{x}.$$

DEFINITION 2.4. For $\alpha \in \mathbb{N}$, the space $\mathcal{H}(K_{\alpha,a,d})$ is a Korobov space on the box $[-a, a]^d$, which is an RKHS with the inner product

$$\langle f, g \rangle_{K_{\alpha,a,d}} := \sum_{\mathbf{h} \in \mathbb{Z}^d} \widehat{f}_{\alpha,d}(\mathbf{h}) \overline{\widehat{g}_{\alpha,d}(\mathbf{h})} r_{\alpha,a,d}(\mathbf{h})^2,$$

and the reproducing kernel

$$\begin{aligned} K_{\alpha,a,d}(\mathbf{x}, \mathbf{y}) &:= \sum_{\mathbf{h} \in \mathbb{Z}^d} r_{\alpha,a,d}(\mathbf{h})^{-2} \varphi_{\alpha,d,\mathbf{h}}(\mathbf{x}) \overline{\varphi_{\alpha,d,\mathbf{h}}(\mathbf{y})} \\ &= \prod_{j=1}^d \left(\frac{1}{(2a)^2} + \frac{(-1)^{\alpha+1}}{(2\alpha)!} \widetilde{B}_{\alpha,2\alpha}(x_j - y_j - a) \right), \end{aligned}$$

where

$$(2.1) \quad r_{\alpha,a,d}(\mathbf{h}) := \prod_{j=1}^d r_{\alpha,a}(h_j), \quad r_{\alpha,a}(h_j) = \begin{cases} \sqrt{2a}, & \text{for } h_j = 0, \\ |\pi h_j / a|^\alpha, & \text{for } h_j \neq 0. \end{cases}$$

Similar to the Korobov space on the unit cube, $\mathcal{H}(K_{\alpha,a,d})$ consists of all functions that are C^α -periodic on $[-a, a]^d$, and the inner product of $\mathcal{H}(K_{\alpha,a,d})$ has the following form

$$\begin{aligned} &\langle f, g \rangle_{K_{\alpha,a,d}} \\ &= \sum_{u \subset \{1:d\}} \int_{[-a,a]^{|u|}} \left(\int_{[-a,a]^{d-|u|}} \partial_u^\alpha f(\mathbf{x}) d\mathbf{x}_{-u} \right) \left(\int_{[-a,a]^{d-|u|}} \partial_u^\alpha g(\mathbf{x}) d\mathbf{x}_{-u} \right) d\mathbf{x}_u. \end{aligned}$$

2.3. Density estimation in RKHS. In this subsection, with an abuse of notation, we recall the theory of density estimation in general RKHS as presented in [20]. Let $(\Omega, \mathcal{F}, \mathbb{P})$ be a probability space and (D, \mathcal{B}) be a measurable space. Suppose independent random vectors $Y_1, \dots, Y_M : \Omega \rightarrow D$ follow an identical distribution defined by a density $f \in \mathcal{H}(K)$ with respect to a measure μ on \mathcal{B} , where $K : D \times D \rightarrow \mathbb{R}$ is a reproducing kernel. The kernel method in [20] consider the estimator

$$(2.2) \quad f_{\mathbf{Y}}^\lambda(\cdot) = \sum_{k=1}^N c_k(\omega) K(x_k, \cdot),$$

where N is a positive integer, $X = \{x_1, \dots, x_N\}$ is a preselected point set in D , and the (random) coefficient vector $\mathbf{c}(\omega) := (c_1(\omega), \dots, c_N(\omega))^\top \in \mathbb{R}^N$ depends on the sample set $\mathbf{Y}(\omega) := \{Y_1(\omega), \dots, Y_M(\omega)\}$ and the ‘‘regularization’’ parameter λ . Specifically, if we denote

$$V_N := V_N(X) := \text{span}\{K(x_k, \cdot) | k = 1, \dots, N\} \subset \mathcal{H}(K),$$

then the coefficient vector $\mathbf{c}(\omega)$ can be obtained by solving a variational formulation

$$(2.3) \quad \langle f_{\mathbf{Y}}^\lambda, v \rangle_{L_\mu^2(D)} + \lambda \langle f_{\mathbf{Y}}^\lambda, v \rangle_K = \frac{1}{M} \sum_{m=1}^M v(Y_m) \quad \text{for all } v \in V_N.$$

It is equivalent to solving the linear system

$$(2.4) \quad A\mathbf{c} = \mathbf{b},$$

where the matrix $A \in \mathbb{R}^{N \times N}$ is given by $A_{j,k} = \langle K(x_j, \cdot), K(x_k, \cdot) \rangle_{L_\mu^2(D)} + \lambda K(x_j, x_k)$ for $j, k = 1, \dots, N$, and the vector $\mathbf{b} \in \mathbb{R}^N$ is given by $b_j = \frac{1}{M} \sum_{m=1}^M K(x_j, Y_m)$ for $j = 1, \dots, N$. Remarkably, the formula (2.3) here is a special case of variational formulation (1.2), serving as the foundation for our PSKK method.

In order to analyze the MISE convergence, the kernel K is assumed to admit an $L_\mu^2(D)$ orthonormal expansion

$$K(x, y) = \sum_{l=0}^{\infty} \beta_l \varphi_l(x) \varphi_l(y),$$

where $\{\varphi_l\}_{l=0}^{\infty}$ is an orthonormal system of $L_\mu^2(D)$ and $(\beta_l)_{l=0}^{\infty} \subset (0, \infty)$. With this assumption, the inner product for $\mathcal{H}(K)$ is given by

$$\langle f, g \rangle_K = \sum_{l=0}^{\infty} \beta_l^{-1} \langle f, \varphi_l \rangle_{L_\mu^2(D)} \langle g, \varphi_l \rangle_{L_\mu^2(D)}.$$

The continuum scale of nested Hilbert spaces related to $\mathcal{H}(K)$ is also introduced. For $\tau > 0$, denote

$$\mathcal{N}^\tau(K) := \left\{ v \in L_\mu^2 : \|v\|_{\mathcal{N}^\tau(K)}^2 = \sum_{l=0}^{\infty} \beta_l^{-\tau} \left| \langle v, \varphi_l \rangle_{L_\mu^2(D)} \right|^2 < \infty \right\}.$$

Denote the normed sapce

$$\mathcal{N}^{-\tau}(K) := \left\{ \Psi : \mathcal{N}^\tau(K) \rightarrow \mathbb{R}, \Psi(v) = \sum_{l=0}^{\infty} \Psi_l \langle v, \varphi_l \rangle_{L_\mu^2(D)} : \|\Psi\|_{\mathcal{N}^{-\tau}(K)} < \infty \right\},$$

where $\|\Psi\|_{\mathcal{N}^{-\tau}(K)}^2 := \sum_{l=0}^{\infty} \beta_l^\tau |\Psi_l|^2$. By [20, proposition 2.1], $\mathcal{N}^{-\tau}(K)$ can be regarded as the dual space of $\mathcal{N}^\tau(K)$. These spaces will be used in Section 3 to derive an upper bound for the MISE.

3. Density estimation in Korobov spaces on a box. In this section we apply the estimation (2.3) to the density function $f \in \mathcal{H}(K_{\alpha,a,d})$ with $a \geq 0.5$. Under these settings, we have $D = [-a, a]^d$ and μ is the Lebesgue measure on $[-a, a]^d$. The orthogonal system $\{\varphi_l\}$ is replaced by $\{\varphi_{\alpha,a,d,\mathbf{h}}\}$ and the coefficients $\{\beta_l\}$ are replaced by $\{r_{\alpha,a,d}(\mathbf{h})^{-2}\}$. Thus the pre-selected point set $X = \{\mathbf{x}_1, \dots, \mathbf{x}_N\} \subset [-a, a]^d$ and

$$(3.1) \quad V_N = V_N(X) = \text{span} \{K_{\alpha,a,d}(\mathbf{x}_k, \cdot) : k = 1, \dots, N\}.$$

Now let $P_N : \mathcal{H}(K_{\alpha,a,d}) \rightarrow V_N$ be the $\mathcal{H}(K_{\alpha,a,d})$ -orthogonal projection and denote

$$\Delta_{\mathbf{Y}}(v) := \frac{1}{M} \sum_{m=1}^M v(Y_m), \quad F(v) := \int_{[-a,a]^d} v(\mathbf{x}) f(\mathbf{x}) d\mathbf{x}.$$

We recall [20, Theorem 3.6] to bound the MISE.

THEOREM 3.1. *Let $f \in \mathcal{H}(K_{\alpha,a,d})$ be the target density function and let $f_{\mathbf{Y}}^\lambda \in V_N$ satisfy (2.3). Suppose that for some $\tau \in (0, 1]$ we have $\Delta_{\mathbf{Y}}, F \in \mathcal{N}^{-\tau}(K_{\alpha,a,d})$ and that f satisfies $\langle K_\tau(\cdot, \cdot), f \rangle_{L^2([-a,a]^d)} < \infty$ with*

$$(3.2) \quad K_\tau(\mathbf{x}, \mathbf{y}) = \sum_{\mathbf{h} \in \mathbb{Z}^d} r_{\alpha,a,d}(\mathbf{h})^{-2\tau} \varphi_{a,d,\mathbf{h}}(\mathbf{x}) \overline{\varphi_{a,d,\mathbf{h}}(\mathbf{y})},$$

where $r_{\alpha,a,d}(\mathbf{h})$ is defined by (2.1). Then we have the MISE bound

$$\begin{aligned} & \mathbb{E} \left[\int_{[-a,a]^d} |f_{\mathbf{Y}}^\lambda(\mathbf{x}) - f(\mathbf{x})|^2 d\mathbf{x} \right] \\ & \leq \|P_N f - f\|_{L^2([-a,a]^d)}^2 + \lambda \|f\|_{K_{\alpha,a,d}}^2 + \frac{\langle K_\tau(\cdot, \cdot), f \rangle_{L^2([-a,a]^d)}}{M\lambda\tau}. \end{aligned}$$

To get a bound on MISE, it remains to determine the range of τ and to handle the term $\|P_N f - f\|_{L^2([-a,a]^d)}$.

3.1. The lower bound for τ . We first derive a lower bound for τ such that the conditions in Theorem 3.1 are satisfied. To establish this bound, we require the following three technical lemmas. The proofs of these lemmas are analogous to the proof of [20, Proposition 4.2], with the additional observation that $\varphi_{a,d,\mathbf{h}}(\mathbf{x}) \leq (2a)^{-\frac{d}{2}}, \forall \mathbf{x} \in [-a,a]^d$ and that f is a density function on $[-a,a]^d$. We provide these proofs in detail in Appendix A, B and C.

LEMMA 3.2. *If $\tau > \frac{1}{2\alpha}$, then for any $\mathbf{x} \in [-a,a]^d$, the point evaluation functional $\delta_{\mathbf{x}}(v) = v(\mathbf{x})$ satisfies $\delta_{\mathbf{x}} \in \mathcal{N}^{-\tau}(K_{\alpha,a,d})$.*

LEMMA 3.3. *If $\tau > \frac{1}{2\alpha}$, then $F \in \mathcal{N}^{-\tau}(K_{\alpha,a,d})$.*

LEMMA 3.4. *For $\tau > \frac{1}{2\alpha}$, let $K_\tau(\mathbf{x}, \mathbf{y})$ be defined in (3.2), then we have*

$$\langle K_\tau(\cdot, \cdot), f(\cdot) \rangle_{L^2([-a,a]^d)} = (2a)^{-d} \left((2a)^{-\tau} + 2 \left(\frac{a}{\pi} \right)^{2\alpha\tau} \zeta(2\alpha\tau) \right)^d < \infty,$$

where $\zeta(s) := \sum_{n=1}^{\infty} \frac{1}{n^s}$ for $s > 1$ is the Riemann zeta function.

Therefore, the conditions in Theorem 3.1 hold if $\tau > \frac{1}{2\alpha}$.

3.2. Error bound for the projection. In this subsection we focus on the L^2 error between f and $P_N f$. We note that $\mathcal{H}(K_{\alpha,a,d}) \subset L^2([-a,a]^d)$ since all functions in $\mathcal{H}(K_{\alpha,a,d})$ are continuous and $[-a,a]^d$ is a finite interval. According to [17, Theorem 2], we obtain a lemma regarding the optimality of P_N .

LEMMA 3.5. *Let $A_N : \mathcal{H}(K_{\alpha,a,d}) \rightarrow \mathcal{H}(K_{\alpha,a,d})$ be an algorithm such that $A_N(\phi) = A_N(\phi(\mathbf{x}_1), \dots, \phi(\mathbf{x}_N))$ only depends on $\phi(\mathbf{x}_1), \dots, \phi(\mathbf{x}_N)$ for all $\phi \in \mathcal{H}(K_{\alpha,a,d})$. Then*

$$\sup_{\|\phi\|_{K_{\alpha,a,d}} \leq 1} \|P_N \phi - \phi\|_{L^2([-a,a]^d)} \leq \sup_{\|\phi\|_{K_{\alpha,a,d}} \leq 1} \|A_N(\phi) - \phi\|_{L^2([-a,a]^d)}$$

Based on this lemma, we only need to find an algorithm A_N over $\mathcal{H}(K_{\alpha,a,d})$ such that $\|A_N(g) - g\|_{L^2([-a,a]^d)}$ is small.

Cools et al. [8] developed a lattice algorithm for function h in Korobov spaces over $[0, 1]^d$. The lattice algorithm uses only function values at lattice points and can converge to h rapidly. Now we employ [8, Theorem 3.6] to the Korobov space $\mathcal{H}(K_{\alpha,d})$ and obtain the following lemma.

LEMMA 3.6. *Given integers d, α , and a prime N , a generating vector \mathbf{z}^* can be constructed by the component-by-component (CBC) construction in [8] so that for*

$$Y^* = \left\{ \mathbf{y}_k^* = \left\{ \frac{k\mathbf{z}^*}{N} \right\} : k = 1, \dots, N \right\},$$

where $\{\cdot\}$ denotes the fractional part of each component, the corresponding lattice algorithm $B_N^* : \mathcal{H}(K_{\alpha,d}) \rightarrow \mathcal{H}(K_{\alpha,d})$ in [8] uses only function values at Y^* and satisfies

$$\|h - B_N^*(h)\|_{L^2([0,1]^d)} \leq C_{\alpha,\delta,d} \|h\|_{K_{\alpha,d}} N^{-(\alpha/2-\delta)}, \quad \forall h \in \mathcal{H}(K_{\alpha,d}), \delta \in (0, \alpha/2),$$

where

$$(3.3) \quad C_{\alpha,\delta,d} = \sqrt{2}\kappa^{\alpha-2\delta} \left(\sum_{u \subset \{1:d\}} \max(|u|, 1) \left[2 \left(\frac{1}{2\pi} \right)^{\frac{\alpha}{\alpha-2\delta}} \zeta \left(\frac{\alpha}{\alpha-2\delta} \right) \right]^{|u|} \right)^{2\alpha-4\delta},$$

with $\kappa = \max \left(6, 2.5 + 2^{\frac{2\alpha}{\alpha-2\delta}+1} \right)$ and $\zeta(s) := \sum_{n=1}^{\infty} \frac{1}{n^s}$ for $s > 1$ being the Riemann zeta function.

Now for function $\phi \in \mathcal{H}(K_{\alpha,a,d})$, we consider the transformation $H(\phi)(\mathbf{y}) = h(\mathbf{y}) := \phi(2a\mathbf{y} - a\mathbf{1})$. Then $h \in \mathcal{H}(K_{\alpha,d})$ and

$$\begin{aligned} \|h\|_{K_{\alpha,d}}^2 &= \sum_{u \subset \{1:d\}} \int_{[0,1]^{|u|}} \left(\int_{[0,1]^{d-|u|}} \partial_u^\alpha h(\mathbf{y}) d\mathbf{y}_{-u} \right)^2 d\mathbf{y}_u \\ &= \sum_{u \subset \{1:d\}} (2a)^{(2\alpha+1)|u|-2d} \int_{[-a,a]^{|u|}} \left(\int_{[-a,a]^{d-|u|}} \partial_u^\alpha \phi(\mathbf{x}) d\mathbf{x}_{-u} \right)^2 d\mathbf{x}_u \\ (3.4) \quad &\leq (2a)^{(2\alpha-1)d} \|\phi\|_{K_{\alpha,a,d}}^2. \end{aligned}$$

Let $h_N = B_N^*(h)$ and define an algorithm

$$(3.5) \quad A_N^*(\phi)(\mathbf{x}) = \phi_N(\mathbf{x}) := H^{-1}(h_N)(\mathbf{x}) = h_N \left(\frac{\mathbf{x}}{2a} + \frac{\mathbf{1}}{2} \right).$$

Then A_N^* is an algorithm over $\mathcal{H}(K_{\alpha,a,d})$ that uses only function values on the point set

$$(3.6) \quad X^* := \{\mathbf{x}_k^* = 2a\mathbf{y}_k^* - a\mathbf{1} : k = 1, \dots, N\}.$$

PROPOSITION 3.7. *Let A_N^* and X^* be defined as (3.5) and (3.6), respectively. For any $\phi \in \mathcal{H}(K_{\alpha,a,d})$ and any $\delta \in (0, \alpha/2)$ we have*

$$\|\phi - A_N^*(\phi)\|_{L^2([-a,a]^d)} \leq C_{\alpha,\delta,d} \|\phi\|_{K_{\alpha,a,d}} (2a)^{\alpha d} N^{-\alpha/2+\delta},$$

where $C_{\alpha,\delta,d}$ is defined by (3.3).

The proof of Proposition 3.7 relies on Lemma 3.6 and inequality (3.4). We provide the details in Appendix D.

Combing Lemma 3.5 and Proposition 3.7, we have the following bound for the projection error.

PROPOSITION 3.8. *Let N be a prime number and let $V_N = V_N(X^*)$ with X^* defined by (3.6). For any $\phi \in \mathcal{H}(K_{\alpha,a,d})$ and any $\delta \in (0, \alpha/2)$, we have*

$$\|P_N \phi - \phi\|_{L^2([-a,a]^d)} \leq C_{\alpha,\delta,d} \|\phi\|_{K_{\alpha,a,d}} (2a)^{\alpha d} N^{-(\alpha/2-\delta)}.$$

By incorporating the results of Lemma 3.4 and Proposition 3.8 into Theorem 3.1, we obtain an upper bound for the MISE.

THEOREM 3.9. *Given $d, \alpha \in \mathbb{N}$ and $a \geq 0.5$. Assume that the target density $f \in \mathcal{H}(K_{\alpha,a,d})$. Let N be a prime number and let $V_N = V_N(X^*)$ with X^* defined by (3.6). Let $f_{\mathbf{Y}}^\lambda \in V_N(X^*)$ satisfy (2.3). For any $\tau \in (1/(2\alpha), 1]$, $\lambda \in (0, 1)$ and $\delta \in (0, \alpha/2)$, we have*

$$\begin{aligned} & \mathbb{E} \left[\int_{[-a,a]^d} |f_{\mathbf{Y}}^\lambda(\mathbf{x}) - f(\mathbf{x})|^2 d\mathbf{x} \right] \\ & \leq C_{\alpha,\delta,d}^2 \frac{(2a)^{2\alpha d} \|f\|_{K_{\alpha,a,d}}^2}{N^{\alpha-2\delta}} + \lambda \|f\|_{K_{\alpha,a,d}}^2 + \frac{\left((2a)^{-\tau-1} + \frac{1}{a} \left(\frac{a}{\pi} \right)^{2\alpha\tau} \zeta(2\alpha\tau) \right)^d}{M\lambda^\tau}, \end{aligned}$$

where $C_{\alpha,\delta,d}$ is defined in (3.3).

Remark 3.10. Theorem 3.9 establishes the MISE bound for the estimator when the density function f lies in the scaled Korobov space, explicitly characterizing its dependence on N , λ , M , and the scaling parameter a . In Section 4, we will transform the density function f on \mathbb{R}^d into its wrapped version \tilde{f} within the scaled Korobov space, thereby deriving the corresponding MISE bound via Theorem 3.9.

4. Density estimation on \mathbb{R}^d . In this section, we consider the density function f defined over \mathbb{R}^d . More precisely, we focus on functions with continuous mixed partial derivatives satisfying the following exponential decay condition.

DEFINITION 4.1 (Exponential decay condition up to order α). *For any function $h : \mathbb{R}^d \rightarrow \mathbb{R}$ with continuous mixed partial derivatives up to order α in each variable, we say h satisfies the exponential decay condition up to order α if*

$$\|h\|_{\alpha,\beta,p,q} := \sup_{\mathbf{x} \in \mathbb{R}^d, \tau \in \{0:\alpha\}^d} \left| \exp(\beta \|\mathbf{x}\|_p^q) h^{(\tau)}(\mathbf{x}) \right| < \infty,$$

for some $\beta > 0$, $1 \leq p \leq \infty$ and $1 \leq q < \infty$, where $\|\mathbf{x}\|_p$ is the ℓ_p -norm of \mathbf{x} .

DEFINITION 4.2. *Given $\alpha \in \mathbb{N}$, $\beta > 0$, $1 \leq p \leq \infty$ and $1 \leq q < \infty$, let $S_{\beta,p,q}^\alpha$ be the collection of all function f that has continuous mixed partial derivatives up to order α in each variable such that $\|f\|_{\alpha,\beta,p,q} < \infty$ and the norm*

$$\|f\|_\alpha^2 := \sum_{u \subset \{1:d\}} \int_{\mathbb{R}^{|u|}} \left(\int_{\mathbb{R}^{d-|u|}} |\partial_u^\alpha f(\mathbf{x})| d\mathbf{x}_{-u} \right)^2 d\mathbf{x}_u,$$

is finite.

Remark 4.3. The function space $S_{\beta,p,q}^\alpha$ includes common density functions such as Gaussian mixtures (with $q = 2$) and logistic distributions (with $q = 1$), where α can be any positive integer for both.

Now we propose our PSKK method for density function $f \in S_{\beta,p,q}^\alpha$ as follows. Given M independent random vectors Y_1, \dots, Y_M whose density function is f , we

consider an unspecified parameter $a \geq 0.5$ and denote \tilde{Y}_m as the remainder of Y_m modulo $2a$ for all $1 \leq m \leq M$. More specifically, for each $1 \leq m \leq M$, we transform the random vector $Y_m = (Y_{m,1}, \dots, Y_{m,d})^\top$ into $\tilde{Y}_m = (\tilde{Y}_{m,1}, \dots, \tilde{Y}_{m,d})^\top$ by defining

$$\tilde{Y}_{m,j} = (Y_{m,j} \bmod 2a) - a \in [-a, a),$$

for all $1 \leq j \leq d$. Then $\tilde{Y}_1, \dots, \tilde{Y}_M$ are iid random vectors taking values in $[-a, a]^d$. Given the condition that $\tilde{Y}_1 = Y_1 - 2a\mathbf{k}$ for some $\mathbf{k} \in \mathbb{Z}^d$, the conditional density function of \tilde{Y}_1 is $f(\mathbf{x} + 2a\mathbf{k})/\mathbb{P}(\tilde{Y}_1 = Y_1 - 2a\mathbf{k})$. It follows from the law of total probability that the density function of \tilde{Y}_1 is $\tilde{f}(\mathbf{x}) = \sum_{\mathbf{k} \in \mathbb{Z}^d} f(\mathbf{x} + 2a\mathbf{k})$, $\forall \mathbf{x} \in [-a, a]^d$. If we extend \tilde{f} to $[-a, a]^d$ with the same formula

$$(4.1) \quad \tilde{f}(\mathbf{x}) = \sum_{\mathbf{k} \in \mathbb{Z}^d} f(\mathbf{x} + 2a\mathbf{k}), \quad \forall \mathbf{x} \in [-a, a]^d,$$

then \tilde{f} is periodic on $[-a, a]^d$ and continues to serve as the density of \tilde{Y}_1 . Since \tilde{f} satisfies the exponential decay condition up to order α , for every $\boldsymbol{\tau} \in \{0:\alpha\}^d$, we have

$$(4.2) \quad \tilde{f}^{(\boldsymbol{\tau})}(\mathbf{x}) = \sum_{\mathbf{k} \in \mathbb{Z}^d} f^{(\boldsymbol{\tau})}(\mathbf{x} + 2a\mathbf{k}),$$

which is a continuous function on $[-a, a]^d$. So \tilde{f} is C^α -periodic on $[-a, a]^d$, thus belonging to the scaled Korobov space $\mathcal{H}(K_{\alpha,a,d})$.

Remark 4.4. In order to change f into a periodic density function on $[-a, a]^d$, one may define a smooth transformation $T : [-a, a]^d \rightarrow \mathbb{R}^d$ such that $Y_1 = T(Z_1)$ for some random vector Z_1 . The density of Z_1 is then given by $g(\mathbf{z}) = f(T(\mathbf{z})) |\det(DT(\mathbf{z}))|$, where $DT(\mathbf{z})$ is the Jacobian of T . Although periodization in quasi-Monte Carlo methods (e.g., polynomial transformations [21] or trigonometric transformations [22, 33]) can construct T to yield periodic g for densities supported on $[0, 1]^d$, extending such smooth transformations to \mathbb{R}^d is hindered by the unbounded domain, rendering T practically infeasible. Consequently, we consider the modulo operation to periodize the density function, which, despite losing partial sample information, offers greater operational simplicity.

We perform the density estimation (2.3) on \tilde{f} in the Korobov space $\mathcal{H}(K_{\alpha,a,d})$ and obtain an estimator $\tilde{f}_{\tilde{\mathbf{Y}}}^\lambda$, where $\tilde{\mathbf{Y}} := \{\tilde{Y}_1, \dots, \tilde{Y}_M\}$. Finally, the PSKK estimator of f is set to be

$$(4.3) \quad f_{\tilde{\mathbf{Y}}}^\lambda(\mathbf{x}) := \begin{cases} \max\{\tilde{f}_{\tilde{\mathbf{Y}}}^\lambda(\mathbf{x}), 0\}, & \text{for } \mathbf{x} \in [-a, a]^d, \\ 0, & \text{for } \mathbf{x} \in \mathbb{R}^d \setminus [-a, a]^d. \end{cases}$$

Note that the estimator (4.3) converts the negative part to 0, which is different from the estimator used in [20].

For the MISE of the PSKK estimator $f_{\tilde{\mathbf{Y}}}^\lambda$, we have

$$(4.4) \quad \begin{aligned} & \mathbb{E} \left[\int_{\mathbb{R}^d} |f_{\tilde{\mathbf{Y}}}^\lambda(\mathbf{x}) - f(\mathbf{x})|^2 d\mathbf{x} \right] \\ & \leq \mathbb{E} \left[\int_{[-a, a]^d} |\tilde{f}_{\tilde{\mathbf{Y}}}^\lambda(\mathbf{x}) - f(\mathbf{x})|^2 d\mathbf{x} \right] + \int_{\mathbb{R}^d \setminus [-a, a]^d} |f(\mathbf{x})|^2 d\mathbf{x} \\ & \leq 2\|f - \tilde{f}\|_{L^2([-a, a]^d)}^2 + 2\mathbb{E} \left[\|\tilde{f}_{\tilde{\mathbf{Y}}}^\lambda - \tilde{f}\|_{L^2([-a, a]^d)}^2 \right] + \int_{\mathbb{R}^d \setminus [-a, a]^d} |f(\mathbf{x})|^2 d\mathbf{x}. \end{aligned}$$

Here, the first term on the right hand side of (4.4) measures the L^2 distance between f and \tilde{f} . The second term quantifies the MISE of estimating \tilde{f} in the scaled Korobov space. The third term corresponds to the truncation error caused by restricting the support of f_Y^λ to $[-a, a]^d$. Before bounding these three terms individually, we prove a key technical lemma.

LEMMA 4.5. *Suppose a function g satisfies the exponential decay condition up to order 0, i.e., $\|g\|_{0,\beta,p,q} = \sup_{\mathbf{x} \in \mathbb{R}^d} |\exp(\beta \|\mathbf{x}\|_p^q) g(\mathbf{x})| < \infty$, for some $\beta > 0, 1 \leq p \leq \infty$ and $1 \leq q < \infty$. For $a > 0$, let $\tilde{g}(\mathbf{x}) = \sum_{\mathbf{k} \in \mathbb{Z}^d} g(\mathbf{x} + 2a\mathbf{k})$, $\forall \mathbf{x} \in [-a, a]^d$.*

Then there exists a constant $C_{d,q}$ depending only on d and q such that for any $a \geq \beta^{-\frac{1}{q}}$ and $\mathbf{x} \in [-a, a]^d$, the following inequality holds

$$(4.5) \quad |g(\mathbf{x}) - \tilde{g}(\mathbf{x})| \leq C_{d,q} \|g\|_{0,\beta,p,q} e^{-\beta a^q}.$$

Proof. For any $\mathbf{x} \in [-a, a]^d$, we have

$$\begin{aligned} |g(\mathbf{x}) - \tilde{g}(\mathbf{x})| &\leq \sum_{\mathbf{k} \in \mathbb{Z}^d \setminus \{\mathbf{0}\}} |g(\mathbf{x} + 2a\mathbf{k})| \\ &\leq \|g\|_{0,\beta,p,q} \sum_{\mathbf{k} \in \mathbb{Z}^d \setminus \{\mathbf{0}\}} \exp(-\beta \|\mathbf{x} + 2a\mathbf{k}\|_p^q) \\ &\leq \|g\|_{0,\beta,p,q} \sum_{\mathbf{k} \in \mathbb{Z}^d \setminus \{\mathbf{0}\}} \exp(-\beta \|\mathbf{x} + 2a\mathbf{k}\|_\infty^q) \\ &\leq \|g\|_{0,\beta,p,q} \sum_{w=1}^{\infty} \sum_{\|\mathbf{k}\|_\infty = w} \exp(-\beta [(2w-1)a]^q) \\ &= \|g\|_{0,\beta,p,q} e^{-\beta a^q} \sum_{w=1}^{\infty} ((2w+1)^d - (2w-1)^d) e^{-\beta a^q ((2w-1)^q - 1)} \\ &\leq \|g\|_{0,\beta,p,q} e^{-\beta a^q} \sum_{w=1}^{\infty} ((2w+1)^d - (2w-1)^d) e^{-((2w-1)^q - 1)}, \end{aligned}$$

where the last inequality uses the condition $\beta a^q \geq 1$. Taking

$$C_{d,q} := \sum_{w=1}^{\infty} ((2w+1)^d - (2w-1)^d) e^{-((2w-1)^q - 1)} < \infty,$$

we obtain (4.5). \square

Lemma 4.5 yields upper bounds for $\|f - \tilde{f}\|_{L^2([-a,a]^d)}^2$ and $\|\tilde{f}\|_{K_{\alpha,a,d}}$.

COROLLARY 4.6. *Suppose $f \in S_{\beta,p,q}^\alpha$ for some $\alpha \in \mathbb{N}, \beta > 0, 1 \leq p \leq \infty$ and $1 \leq q < \infty$. Let \tilde{f} be defined in (4.1) and let $C_{d,q}$ be the constant in Lemma 4.5. For any $a \geq \beta^{-\frac{1}{q}}$, we have*

$$\|f - \tilde{f}\|_{L^2([-a,a]^d)}^2 \leq C_{d,q}^2 \|f\|_{0,\beta,p,q}^2 (2a)^d e^{-2\beta a^q}.$$

COROLLARY 4.7. *Suppose $f \in S_{\beta,p,q}^\alpha$ for some $\alpha \in \mathbb{N}, \beta > 0, 1 \leq p \leq \infty$ and $1 \leq q < \infty$. Let \tilde{f} be defined in (4.1) and let $C_{d,q}$ be the constant in Lemma 4.5. For any $a \geq \max\{\beta^{-\frac{1}{q}}, 0.5\}$, we have*

$$(4.6) \quad \|\tilde{f}\|_{K_{\alpha,a,d}}^2 \leq 2\|f\|_\alpha^2 + 2C_{d,q}^2 \|f\|_{\alpha,\beta,p,q}^2 (2\sqrt{2}a)^{2d} e^{-2\beta a^q}.$$

Proof. Let $g(\mathbf{x}) := \tilde{f}(\mathbf{x}) - f(\mathbf{x})$ for $\mathbf{x} \in [-a, a]^d$. According to Lemma 4.5, for any $a \geq \max\{\beta^{-\frac{1}{q}}, 0.5\}$, $\boldsymbol{\tau} \in \{0:\alpha\}^d$, and $\mathbf{x} \in [-a, a]^d$, we have

$$|g(\boldsymbol{\tau})(\mathbf{x})| \leq C_{d,q} \|f(\boldsymbol{\tau})\|_{0,\beta,p,q} e^{-\beta a^q} \leq C_{d,q} \|f\|_{\alpha,\beta,p,q} e^{-\beta a^q}.$$

We aim to bound $\|\tilde{f}\|_{K_{\alpha,a,d}} = \|f + g\|_{K_{\alpha,a,d}}$. Although f and g may not lie in the Korobov space, we can still compute their Korobov norm, and the triangle inequality yields

$$\|\tilde{f}\|_{K_{\alpha,a,d}} \leq \|f\|_{K_{\alpha,a,d}} + \|g\|_{K_{\alpha,a,d}} \leq \|f\|_{\alpha} + \|g\|_{K_{\alpha,a,d}}.$$

Note that

$$\begin{aligned} \|g\|_{K_{\alpha,a,d}}^2 &= \sum_{u \subset \{1:d\}} \int_{[-a,a]^{|u|}} \left(\int_{[-a,a]^{d-|u|}} \partial_u^\alpha g(\mathbf{x}) d\mathbf{x}_{-u} \right)^2 d\mathbf{x}_u \\ &\leq \sum_{u \subset \{1:d\}} \int_{[-a,a]^{|u|}} \left(\int_{[-a,a]^{d-|u|}} C_{d,q} \|f\|_{\alpha,\beta,p,q} e^{-\beta a^q} d\mathbf{x}_{-u} \right)^2 d\mathbf{x}_u \\ &= C_{d,q}^2 \|f\|_{\alpha,\beta,p,q}^2 e^{-2\beta a^q} \sum_{u \subset \{1:d\}} (2a)^{2d-|u|} \\ &\leq C_{d,q}^2 \|f\|_{\alpha,\beta,p,q}^2 2^d (2a)^{2d} e^{-2\beta a^q}. \end{aligned}$$

So (4.6) follows from the inequality $(x + y)^2 \leq 2x^2 + 2y^2$. \square

To analyze the third term in (4.4), we recall [27, Proposition 8] as follows.

PROPOSITION 4.8. *Suppose an integrand function g satisfies the exponential decay condition up to order 0, i.e., $\|g\|_{0,\beta,p,q} = \sup_{\mathbf{x} \in \mathbb{R}^d} |\exp(\beta \|\mathbf{x}\|_p^q) g(\mathbf{x})| < \infty$, for some $\beta > 0, 1 \leq p \leq \infty$ and $1 \leq q < \infty$. Then for any $a > \beta^{-\frac{1}{q}}$ we have*

$$\left| \int_{\mathbb{R}^d \setminus [-a,a]^d} g(\mathbf{x}) d\mathbf{x} \right| \leq \frac{2^d d}{\beta^{d/q} q} [d/q]! \|g\|_{0,\beta,p,q} (\beta a^q)^{d/q-1} \exp(-\beta a^q).$$

Combining Theorem 3.9, Corollary 4.6, Corollary 4.7, along with Proposition 4.8, we arrive at the following theorem.

THEOREM 4.9. *Given $d, \alpha \in \mathbb{N}$. Assume that the target density $f \in S_{\beta,p,q}^\alpha$ for some $\beta > 0, 1 \leq p \leq \infty$ and $1 \leq q < \infty$. For $\epsilon \in (0, 2 - 1/\alpha)$, take $\tau^* = 1/(2\alpha) + \epsilon/2$, $\lambda^* = \mathcal{O}(M^{-1/(1+\tau^*)})$, and prime number $N^* = \mathcal{O}(M^{1/(\alpha-\epsilon)})$. For any $\eta > 0$, let $a^* = \left[\frac{1}{2\beta} \log(\eta M) \right]^{\frac{1}{q}}$. Denote $\|f\|_{\max} := \max\{\|f\|_{\alpha,\beta,p,q}, \|f\|_{\alpha}\}$ and let $V_{N^*} = V_{N^*}(X^*)$ with X^* defined in (3.6). Then there exists a constant $C = C(\alpha, \beta, \eta, d, q, \epsilon)$ depending only on $\alpha, \beta, \eta, d, q$ and ϵ such that for $M \geq \max\{e^2/\eta, e^{2^{1-q}\beta}/\eta\}$ and the PSKK estimator f_Y^λ in (4.3), we have*

$$(4.7) \quad \mathbb{E} \left[\int_{\mathbb{R}^d} |f_Y^\lambda(\mathbf{x}) - f(\mathbf{x})|^2 d\mathbf{x} \right] \leq C \|f\|_{\max}^2 M^{-\frac{1}{1+1/(2\alpha)+\epsilon}}.$$

Proof. Since $\|f\|_{0,\beta,p,q} \leq \|f\|_{\alpha,\beta,p,q} < \infty$, we have $f \in L^2(\mathbb{R}^d)$ and

$$\|f\|_{0,2\beta,p,q}^2 = \sup_{\mathbf{x} \in \mathbb{R}^d} |\exp(2\beta \|\mathbf{x}\|_p^q) f(\mathbf{x})|^2 = \|f\|_{0,\beta,p,q}^2 < \infty.$$

According to Proposition 4.8, for $a > (2\beta)^{-1/q}$, we have

$$(4.8) \quad \begin{aligned} \int_{\mathbb{R}^d \setminus [-a, a]^d} |f(\mathbf{x})|^2 d\mathbf{x} &\leq \frac{2^d d}{(2\beta)^{d/q} q} [d/q]! \|f\|_{0,\beta,p,q}^2 (2\beta a^q)^{d/q-1} \exp(-2\beta a^q) \\ &\leq C_{\beta,d,q} \|f\|_{0,\beta,p,q}^2 (2a)^d \exp(-2\beta a^q), \end{aligned}$$

where $C_{\beta,d,q}$ is a constant depending only on d, β and q . Substituting inequality (4.8) and the results of Theorem 3.9, Corollary 4.6, and Corollary 4.7, into inequality (4.4), we obtain that for any $\delta \in (0, \alpha/2)$, $\tau \in (1/(2\alpha), 1]$, $\lambda \in (0, 1)$ and $a \geq \max\{\beta^{-\frac{1}{q}}, 0.5\}$,

$$(4.9) \quad \begin{aligned} &\mathbb{E} \left[\int_{\mathbb{R}^d} |f_{\hat{\mathbf{Y}}}^\lambda(\mathbf{x}) - f(\mathbf{x})|^2 d\mathbf{x} \right] \\ &\leq 2C_{d,q}^2 \|f\|_{0,\beta,p,q}^2 (2a)^d e^{-2\beta a^q} + \frac{2 \left((2a)^{-\tau-1} + \frac{1}{a} \left(\frac{a}{\pi} \right)^{2\alpha\tau} \zeta(2\alpha\tau) \right)^d}{M\lambda^\tau} \\ &\quad + 4\lambda \left(\|f\|_\alpha^2 + C_{d,q}^2 \|f\|_{\alpha,\beta,p,q}^2 (2\sqrt{2}a)^{2d} e^{-2\beta a^q} \right) \\ &\quad + 4C_{\alpha,\delta,d}^2 \frac{(2a)^{2\alpha d}}{N^{\alpha-2\delta}} \left(\|f\|_\alpha^2 + C_{d,q}^2 \|f\|_{\alpha,\beta,p,q}^2 (2\sqrt{2}a)^{2d} e^{-2\beta a^q} \right) \\ &\quad + C_{\beta,d,q} \|f\|_{0,\beta,p,q}^2 (2a)^d \exp(-2\beta a^q), \end{aligned}$$

where $C_{\alpha,\delta,q}$ and $C_{d,q}$ are constants defined in (3.3) and Lemma 4.5, respectively. Note that the condition $M \geq \max\{e^2/\eta, e^{2^{1-q}\beta}/\eta\}$ ensures $a^* \geq \max\{\beta^{-\frac{1}{q}}, 0.5\}$. By substituting the value of a^* into inequality 4.9, we obtain that there exists a constant $C' = C'(\alpha, \beta, \delta, \tau, d, q)$ depending only on $\alpha, \beta, \delta, \tau, d$ and q such that

$$(4.10) \quad \begin{aligned} &\mathbb{E} \left[\int_{\mathbb{R}^d} |f_{\hat{\mathbf{Y}}}^\lambda(\mathbf{x}) - f(\mathbf{x})|^2 d\mathbf{x} \right] \\ &\leq C' \|f\|_{\max}^2 \left[\frac{[\log(\eta M)]^{\frac{d}{q}}}{\eta M} + \frac{[\log(\eta M)]^{\frac{2\alpha d}{q}}}{N^{\alpha-2\delta}} \left(1 + \frac{[\log(\eta M)]^{\frac{2d}{q}}}{\eta M} \right) \right. \\ &\quad \left. + \lambda \left(1 + \frac{[\log(\eta M)]^{\frac{2d}{q}}}{\eta M} \right) + \frac{[\log(\eta M)]^{\frac{(2\alpha\tau-1)d}{q}}}{M\lambda^\tau} \right]. \quad \square \end{aligned}$$

Taking $\delta = \epsilon/2$ and plugging the values of τ^* , λ^* and N^* into inequality (4.10), we obtain inequality (4.7).

Remark 4.10. Theorem 4.9 establishes that, with suitable parameter choices, the PSKK estimator achieves an MISE convergence rate of $\mathcal{O}(M^{-1/(1+1/(2\alpha)+\epsilon)})$ for arbitrarily small $\epsilon > 0$. This matches the convergence rate obtained in [20], while extending its applicability to \mathbb{R}^d density estimation.

5. Implementing the PSKK method. We outline our PSKK method as Algorithm 5.1. First, set the theoretical parameters mentioned in Theorem 4.9. Second, preprocess the data by applying modulo reduction into $[-a, a]^d$ and use the CBC algorithm in [7] to generate lattice points. Third, numerically solve the linear system (2.4). Notably, when using lattice points to construct X^* in (3.6), the matrix A in (2.4) exhibits a circulant matrix structure that enables efficient computation. The detailed calculation of A is provided in Appendix E. Finally, we obtain the PSKK estimator as in (4.3).

Algorithm 5.1 Periodic scaled Korobov kernel method

Require: M observed samples $Y_1, \dots, Y_M \in \mathbb{R}^d$. Prior knowledge that $f \in S_{\beta,p,q}^\alpha$ for some $\alpha \in \mathbb{N}, \beta > 0, 1 \leq p \leq \infty$ and $1 \leq q < \infty$.

Select $\epsilon \in (0, 2 - 1/\alpha)$ and $\eta > 0$. Take a prime number N such that $N = \mathcal{O}(M^{\frac{1}{\alpha-\epsilon}})$. Take

$$a = \left(\frac{\log M + \log \eta}{2\beta} \right)^{\frac{1}{q}}, \quad \mathbf{a} = (a, \dots, a)^\top \in \mathbb{R}^d, \quad \lambda = \mathcal{O}(M^{-1/(1+\frac{1}{2\alpha}+\frac{\epsilon}{2})}).$$

For $1 \leq m \leq M$, let $\tilde{Y}_m \in [-a, a]^d$ be the remainder of Y_m modulo $2a$ minus \mathbf{a} . Use the CBC construction in [7] to obtain the lattice point set $Y^* = \{\mathbf{y}_1, \dots, \mathbf{y}_N\} \subset [0, 1]^d$. Take $\mathbf{x}_i := 2a\mathbf{y}_i - \mathbf{a}, i = 1, \dots, N$.

Employ the density estimation in $\mathcal{H}(K_{\alpha,a,d})$ as follows:

Take $A = (A_{j,k})_{1 \leq j, k \leq N}$ and $\mathbf{b} = (b_j)_{1 \leq j \leq N}$ such that

$$A_{j,k} = \langle K_{\alpha,a,d}(\mathbf{x}_j, \cdot), K_{\alpha,a,d}(\mathbf{x}_k, \cdot) \rangle_{L^2([-a,a]^d)} + \lambda K_{\alpha,a,d}(\mathbf{x}_j, \mathbf{x}_k),$$

$$(5.1) \quad b_j = \frac{1}{M} \sum_{m=1}^M K_{\alpha,a,d}(\mathbf{x}_j, \tilde{Y}_m).$$

Solve the linear equation $A\mathbf{c} = \mathbf{b}$.

For the solution $\mathbf{c} = (c_1, \dots, c_N)^\top$, compute the density estimator

$$\tilde{f}_{\mathbf{Y}}^\lambda(\mathbf{x}) = \sum_{n=1}^N c_n K_{\alpha,a,d}(\mathbf{x}_n, \mathbf{x}).$$

return Density estimator

$$f_{\mathbf{Y}}^\lambda(\mathbf{x}) := \begin{cases} \max\{\tilde{f}_{\mathbf{Y}}^\lambda(\mathbf{x}), 0\}, & \text{for } \mathbf{x} \in [-a, a]^d, \\ 0, & \text{for } \mathbf{x} \in \mathbb{R}^d \setminus [-a, a]^d. \end{cases}$$

5.1. Computational complexity of the PSKK method. In this subsection we analyze the overall computational complexity of the PSKK method. First, the CBC construction in [7] for generating the lattice point set Y^* requires $\mathcal{O}(dN \log N)$ operations under product weights in the Korobov space on the unit cube (see [7, Section 4] for detail). Next, constructing the circulant matrix A involves computing its first row elements $A_{1,k}$ for $k = 1, 2, \dots, N$ through kernel evaluations in (E.2) and (E.3), which takes $\mathcal{O}(dN)$ operations. For the vector \mathbf{b} , each entry requires $\mathcal{O}(dM)$ operations according to (5.1), leading to $\mathcal{O}(dMN)$ complexity for all N entries. Finally, solving the linear system $A\mathbf{c} = \mathbf{b}$ via fast Fourier transform leverages the circulant structure of A , requiring $\mathcal{O}(N \log N)$ operations. Therefore, the total computational complexity of the PSKK method is dominated by

$$\mathcal{O}(dN \log N + dN + dMN + N \log N) = \mathcal{O}(dMN).$$

By selecting $N = \mathcal{O}(M^{\frac{1}{\alpha-\epsilon}})$ for some $\epsilon \in (0, 2 - 1/\alpha)$ as in Algorithm 5.1, the complexity reduces to $\mathcal{O}(dM^{1+\frac{1}{\alpha-\epsilon}})$.

Remark 5.1. The PSKK estimator is a function defined on \mathbb{R}^d . Evaluating this estimator at L distinct points requires $\mathcal{O}(dLN) = \mathcal{O}(dLM^{\frac{1}{\alpha-\epsilon}})$ operations after construction.

Remark 5.2. For comparison, the standard KDE method with Scott's rule takes $\mathcal{O}(dLM)$ operations to evaluate L points. The PSKK method achieves a lower complexity than KDE when $L > cM^\rho$ with some positive constant c and $\rho > \frac{1}{\alpha-\epsilon}$, provided $N = \mathcal{O}(M^{\frac{1}{\alpha-\epsilon}})$ as specified in Algorithm 5.1. This condition ensures $\mathcal{O}(dLN + dMN) < \mathcal{O}(dLM)$, demonstrating the computational efficiency of our method for large L . Combined with this low computational complexity, the PSKK method achieves a convergence rate of $\mathcal{O}(M^{-1/(1+1/(2\alpha)+\epsilon)})$, exceeding the $\mathcal{O}(M^{-\frac{4}{d+4}})$ rate of the standard KDE method.

6. Numerical experiments. In this section we perform numerical experiments to validate the theoretical results. All experiments compare the PSKK method with the standard KDE method, and evaluate their performance through the MISE. We provide detailed steps for calculating MISE in Appendix F.

6.1. Example 1: Two-dimensional Gaussian mixture distribution. In this subsection, we examine our PSKK method on the two dimensional Gaussian mixture distribution. In particular, we consider the following density function

$$f(\mathbf{x}) = \frac{1}{9} \sum_{\mu \in \{-2, 0, 2\}^2} \frac{2}{\pi} e^{-2\|\mathbf{x}-\mu\|_2^2}.$$

This density function has nine peaks, with the center of each peak located at the grid points in $\{-2, 0, 2\}^2$. Now we compare the performance of the KDE method and the PSKK method for this density estimation. For the KDE method, we select the conventional Gaussian kernel. For the PSKK method, we chose $\alpha = 2, a = 6, N = 1009$ and $\lambda = 10^{-6}$.

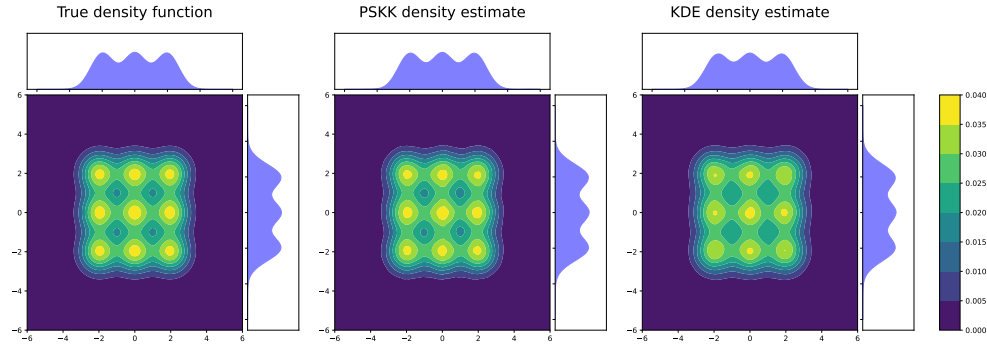


FIG. 6.1. Plot of the density function with marginal distributions for the true density function (left), the PSKK density estimate (middle) and the KDE density estimate (right), based on $M = 10^6$ samples. The PSKK method sets the parameters $\alpha = 2, a = 6, N = 1009$ and $\lambda = 10^{-6}$.

Figure 6.1 shows the true density function (left), the density function estimated by the PSKK method (middle), and the density function estimated by the KDE method

(right). Each method employs $M = 10^6$ independent samples. It is evident that while both methods perform well in estimating the marginal density functions, the PSKK method more effectively captures the modal information of the target density function, particularly in the peaks (yellow regions) and valleys (dark blue regions).

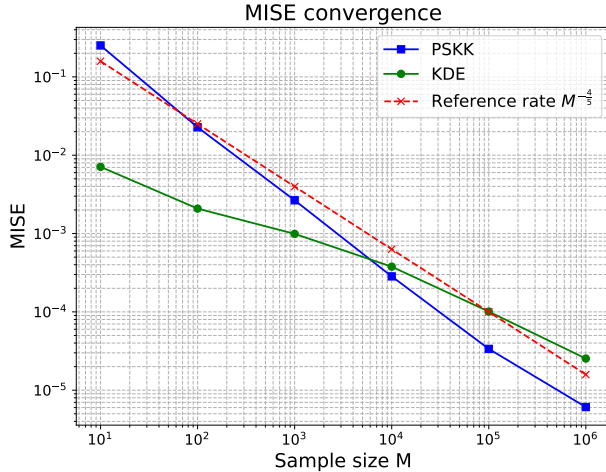


FIG. 6.2. *MISE convergence for the KDE method and the PSKK method (with $\alpha = 2, a = 6, N = 1009$, and $\lambda = 10^{-6}$) in the 2-dimensional Gaussian mixture example.*

We also evaluate the convergence of the MISE for both the KDE and the PSKK methods using sample sizes of $M = 10, 10^2, \dots, 10^6$. As illustrated in Figure 6.2, the PSKK method, under the chosen parameters, exhibits a lower MISE than the KDE method when the sample size exceeds 10^4 , thereby highlighting its superior performance with large samples. Furthermore, when $\alpha = 2$, the PSKK method in this example exhibits a higher MISE convergence rate than the theoretical upper bound of $\mathcal{O}(M^{-\frac{4}{5}})$.

6.2. Example 2: 4-dimensional Gaussian mixture distribution. In this subsection we consider the 4-dimensional Gaussian mixture distribution with the density function

$$f(\mathbf{x}) = \frac{1}{9} \sum_{k=0}^8 \frac{1}{4\pi^2\sigma^4} e^{-\frac{\|\mathbf{x}-\boldsymbol{\mu}_k\|_2^2}{2\sigma^2}},$$

where $\sigma = 0.7$ and for $0 \leq k \leq 8$,

$$\boldsymbol{\mu}_k = \left(\left\{ \frac{k}{9} \right\} - \frac{4}{9}, \left\{ \frac{2k}{9} \right\} - \frac{4}{9}, \left\{ \frac{4k}{9} \right\} - \frac{4}{9}, \left\{ \frac{8k}{9} \right\} - \frac{4}{9} \right)^\top.$$

We aim to verify the convergence rate of the MISE of the PSKK estimator established in Theorem 4.9, using the parameter selection strategy specified in Algorithm 5.1.

Figure 6.3 illustrates the MISE decay for the PSKK method with $a = a(M), N = N(M, \alpha)$ and $\lambda = \lambda(M, \alpha)$ for $\alpha = 2, 3$ as specified in Algorithm 5.1. Specifically, we take $a = \sqrt{(\log M - 1)/2}$ and $\lambda = 0.1M^{-1/(1+1/(2\alpha))}$ for $M = 10, 10^2, \dots, 10^6$. For the selection of N , we choose N to be approximately $3\sqrt{M}$ prime numbers. For

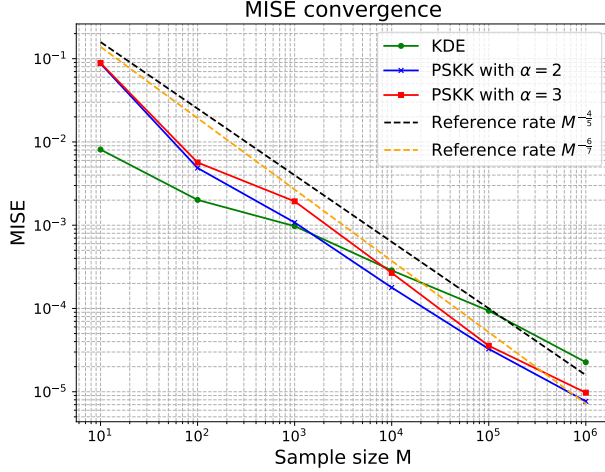


FIG. 6.3. *MISE convergence for the KDE method and the PSKK method (with $\alpha = 2, 3, a = \sqrt{(\log M - 1)/2}, N = \mathcal{O}(3\sqrt{M}),$ and $\lambda = 0.1M^{-1/(1+1/(2\alpha))}$) in the 4-dimensional Gaussian mixture example.*

$M = 10, 10^2, \dots, 10^6$, N is set to 11, 31, 97, 307, 947, 3001, respectively. In both cases of $\alpha = 2$ and $\alpha = 3$, the MISE of the PSKK method exhibits a $\mathcal{O}(M^{-1+1/(2\alpha)})$ decay, which is consistent with our theory. Additionally, we evaluated the MISE decay for the KDE method. The results indicate that, as the sample size M increases, the PSKK method yields a smaller MISE compared to the KDE method.

We also investigate the impact of parameters a, N , and λ on the MISE of the PSKK estimator and conduct similar experiments for higher-dimensional situations. The detailed results of the parameter impact experiments and the higher-dimensional experiments are provided in Appendix G and Appendix H, respectively.

7. Conclusion. In this paper, we propose the periodic scaled Korobov kernel method for density estimation on \mathbb{R}^d under the exponential decay condition. By employing a modulo operation to map samples into the truncated domain $[-a, a]^d$, the PSKK method eliminates the need for compact support or inherent periodicity assumptions required by the kernel method in [20]. Theoretically, we prove that the PSKK estimator achieves a MISE bound of $\mathcal{O}(M^{-1/(1+1/(2\alpha)+\epsilon)})$ for densities with exponential decay up to order α , where $\epsilon > 0$ can be arbitrarily small. Numerical experiments confirm this convergence rate under the parameter choices determined in Theorem 4.9 and demonstrate significant improvements over the standard KDE method, especially for large sample sizes.

Some challenges remain in this work, which we plan to address in future research. First, while the PSKK method achieves a dimension-independent convergence rate of order $\mathcal{O}(M^{-1/(1+1/(2\alpha)+\epsilon)})$, the implied constant in the error bound grows rapidly with increasing dimensionality. Second, the parameter N exhibits strict operational constraints: small N causes non-convergence, whereas large N incurs prohibitive computational costs. This contrasts with [20], where the compact support $[0, 1]^d$ allows for smaller N . Our analysis of the projection error reveals that N scales exponentially with the truncation parameter a , demanding a more efficient kernel approximation in RKHS to resolve the resulting accuracy-complexity trade-off. Third,

the truncation parameter a requires precise calibration—both undersized and oversized a values destabilize the MISE convergence, underscoring the need for adaptive selection strategies.

Appendix A. Proof of Lemma 3.2.

Proof. For $v \in \mathcal{N}^\tau(K_{\alpha,a,d})$, we have

$$\begin{aligned} |\delta_{\mathbf{x}}(v)| &= \left| \sum_{\mathbf{h} \in \mathbb{Z}^d} \widehat{v}_{a,d}(\mathbf{h}) \varphi_{a,d,\mathbf{h}}(\mathbf{x}) \right| \\ &\leq (2a)^{-\frac{d}{2}} \left| \sum_{\mathbf{h} \in \mathbb{Z}^d} \widehat{v}_{a,d}(\mathbf{h}) \right| \\ &\leq (2a)^{-\frac{d}{2}} \left(\sum_{\mathbf{h} \in \mathbb{Z}^d} r_{\alpha,a,d}(\mathbf{h})^{-2\tau} \right)^{\frac{1}{2}} \left(\sum_{\mathbf{h} \in \mathbb{Z}^d} r_{\alpha,a,d}(\mathbf{h})^{2\tau} |\widehat{v}_{a,d}(\mathbf{h})|^2 \right)^{\frac{1}{2}} \\ &= (2a)^{-\frac{d}{2}} \left(\sum_{\mathbf{h} \in \mathbb{Z}^d} r_{\alpha,a,d}(\mathbf{h})^{-2\tau} \right)^{\frac{1}{2}} \|v\|_{\mathcal{N}^\tau(K_{\alpha,a,d})}, \end{aligned}$$

where in the second inequality we use $\varphi_{a,d,\mathbf{h}}(\mathbf{x}) \leq (2a)^{-\frac{d}{2}}, \forall \mathbf{x} \in [-a, a]^d$. Since $\tau > \frac{1}{2\alpha}$, we have

$$\begin{aligned} \sum_{\mathbf{h} \in \mathbb{Z}^d} r_{\alpha,a,d}(\mathbf{h})^{-2\tau} &= \left(r_{\alpha,a}(0)^{-2\tau} + 2 \sum_{h=1}^{\infty} r_{\alpha,a}(h)^{-2\tau} \right)^d \\ &= \left((2a)^{-\tau} + 2 \left(\frac{a}{\pi} \right)^{2\alpha\tau} \zeta(2\alpha\tau) \right)^d < \infty. \end{aligned}$$

Therefore, $\delta_{\mathbf{x}} \in \mathcal{N}^{-\tau}(K_{\alpha,a,d})$ holds for any $\mathbf{x} \in [-a, a]^d$. \square

Appendix B. Proof of Lemma 3.3.

Proof.

$$\begin{aligned} \|F\|_{\mathcal{N}^{-\tau}(K_{\alpha,a,d})}^2 &= \sum_{\mathbf{h} \in \mathbb{Z}^d} r_{\alpha,a,d}(\mathbf{h})^{-2\tau} \left| \int_{[-a,a]^d} f(\mathbf{x}) \varphi_{a,d,\mathbf{h}}(\mathbf{x}) d\mathbf{x} \right|^2 \\ &\leq \sum_{\mathbf{h} \in \mathbb{Z}^d} r_{\alpha,a,d}(\mathbf{h})^{-2\tau} (2a)^{-d} \left| \int_{[-a,a]^d} f(\mathbf{x}) d\mathbf{x} \right|^2 \\ &= (2a)^{-d} \sum_{\mathbf{h} \in \mathbb{Z}^d} r_{\alpha,a,d}(\mathbf{h})^{-2\tau} \\ &= (2a)^{-d} \left((2a)^{-\tau} + 2 \left(\frac{a}{\pi} \right)^{2\alpha\tau} \zeta(2\alpha\tau) \right)^d < \infty, \end{aligned}$$

where in the third equality we use the fact that f is a density function on $[-a, a]^d$. \square

Appendix C. Proof of Lemma 3.4.

Proof.

$$\begin{aligned}
\langle K_\tau(\cdot, \cdot), f(\cdot) \rangle_{L^2([-a, a])} &= (2a)^{-d} \sum_{\mathbf{h} \in \mathbb{Z}^d} r_{\alpha, a, d}(\mathbf{h})^{-2\tau} \int_{[-a, a]^d} f(\mathbf{x}) d\mathbf{x} \\
&= (2a)^{-d} \sum_{\mathbf{h} \in \mathbb{Z}^d} r_{\alpha, a, d}(\mathbf{h})^{-2\tau} \\
&= (2a)^{-d} \left((2a)^{-\tau} + 2 \left(\frac{a}{\pi} \right)^{2\alpha\tau} \zeta(2\alpha\tau) \right)^d < \infty. \quad \square
\end{aligned}$$

Appendix D. Proof of Proposition 3.7.

Proof. For any $\phi \in \mathcal{H}(K_{\alpha, a, d})$, let $h(\mathbf{y}) = H(\phi)(\mathbf{y}) = \phi(2a\mathbf{y} - a\mathbf{1})$. Let $h_N = B_N^*(h)$ with B_N^* defined in Lemma 3.6 and let $\phi_N = A_N^*(\phi)$. Then we have

$$\begin{aligned}
\|\phi - A_N^*(\phi)\|_{L^2([-a, a]^d)}^2 &= \int_{[-a, a]^d} |\phi(\mathbf{x}) - \phi_N(\mathbf{x})|^2 d\mathbf{x} \\
&= \int_{[-a, a]^d} \left| h\left(\frac{\mathbf{x}}{2a} + \frac{\mathbf{1}}{2}\right) - h_N\left(\frac{\mathbf{x}}{2a} + \frac{\mathbf{1}}{2}\right) \right|^2 d\mathbf{x} \\
&= (2a)^d \int_{[0, 1]^d} |h(\mathbf{y}) - h_N(\mathbf{y})|^2 d\mathbf{y},
\end{aligned}$$

According to Lemma 3.6 and inequality (3.4), we have

$$\begin{aligned}
\|\phi - A_N^*(\phi)\|_{L^2([-a, a]^d)} &= (2a)^{d/2} \|h - B_N^*(h)\|_{L^2([0, 1]^d)} \\
&\leq (2a)^{d/2} C_{\alpha, \delta, d} \|h\|_{K_{\alpha, d}} N^{-(\alpha/2 - \delta)} \\
&\leq C_{\alpha, \delta, d} \|\phi\|_{K_{\alpha, a, d}} (2a)^{\alpha d} N^{-(\alpha/2 - \delta)}. \quad \square
\end{aligned}$$

Appendix E. Computing the elements of A . Here we introduce how to calculate A mentioned in Algorithm 5.1 of the form $A = (A_{j, k})_{1 \leq j, k \leq N}$ with

$$(E.1) \quad A_{j, k} = \langle K_{\alpha, a, d}(\mathbf{x}_j, \cdot), K_{\alpha, a, d}(\mathbf{x}_k, \cdot) \rangle_{L^2([-a, a]^d)} + \lambda K_{\alpha, a, d}(\mathbf{x}_j, \mathbf{x}_k).$$

We note that for any $\tau \in \mathbb{N}$, $\tau \geq 2$, the periodic Bernoulli polynomial of degree τ has the following form (see [28] for more details)

$$\tilde{B}_\tau(x) = \frac{-1}{(2\pi i)^\tau} \sum_{h \in \mathbb{Z} \setminus \{0\}} \frac{e^{2\pi i h x}}{h^\tau}, \quad \forall x \in \mathbb{R}.$$

So we have

$$\begin{aligned}
&K_{\alpha, a, d}(\mathbf{x}, \mathbf{y}) \\
&= \prod_{j=1}^d \left(\frac{1}{(2a)^2} + (-1)^{\alpha+1} \frac{\tilde{B}_{a, 2\alpha}(x_j - y_j + a_j)}{(2\alpha)!} \right) \\
(E.2) \quad &= \prod_{j=1}^d \left(\frac{1}{(2a)^2} + \sum_{h \in \mathbb{Z} \setminus \{0\}} \frac{(2a)^{2\alpha-1}}{|2\pi h|^{2\alpha}} \exp\left(2\pi i h \frac{x_j - y_j}{2a}\right) \right).
\end{aligned}$$

Thus

$$\begin{aligned}
& \langle K_{\alpha,a,d}(\mathbf{x}, \cdot), K_{\alpha,a,d}(\mathbf{y}, \cdot) \rangle_{L^2([-a,a])} \\
&= \prod_{j=1}^d \left[\int_{-a}^a \left(\frac{1}{(2a)^2} + \sum_{h \in \mathbb{Z} \setminus \{0\}} \frac{(2a)^{2\alpha-1}}{|2\pi h|^{2\alpha}} \exp\left(2\pi i h \frac{x_j - z_j}{2a}\right) \right) \right. \\
&\quad \left. \times \left(\frac{1}{(2a)^2} + \sum_{h \in \mathbb{Z} \setminus \{0\}} \frac{(2a)^{2\alpha-1}}{|2\pi h|^{2\alpha}} \exp\left(2\pi i h \frac{z_j - y_j}{2a}\right) \right) dz_j \right] \\
&= \prod_{j=1}^d \left((2a)^{-3} + \sum_{h \in \mathbb{Z} \setminus \{0\}} \frac{(2a)^{4\alpha-1}}{|2\pi h|^{4\alpha}} \exp\left(2\pi i h \frac{x_j - y_j}{2a}\right) \right) \\
\text{(E.3)} \quad &= \prod_{j=1}^d \left((2a)^{-3} - (2a)^{4\alpha-1} \frac{\tilde{B}_{4\alpha}((x_j - y_j)/(2a))}{(4\alpha)!} \right).
\end{aligned}$$

Remark E.1. According to (E.2), (E.3) and (E.1), when the point set X^* is taken as scaled lattice points, the matrix A becomes a circular matrix, and thus equation (2.4) can be solved quickly using the fast Fourier transform [12].

Appendix F. Detailed steps for calculating MISE. For the KDE estimator $f_{\mathbf{Y}}^{\text{KDE}}$ based on the sample set $\mathbf{Y} = \{Y_1, \dots, Y_M\}$, the MISE is estimated as

$$\begin{aligned}
\text{MISE}(f_{\mathbf{Y}}^{\text{KDE}}) &:= \mathbb{E} \left[\int_{\mathbb{R}^d} |f_{\mathbf{Y}}^{\text{KDE}}(\mathbf{x}) - f(\mathbf{x})|^2 d\mathbf{x} \right] \\
&\approx \mathbb{E} \left[\int_{[-l,l]^d} |f_{\mathbf{Y}}^{\text{KDE}}(\mathbf{x}) - f(\mathbf{x})|^2 d\mathbf{x} \right] \\
\text{(F.1)} \quad &\approx \frac{(2l)^d}{S} \sum_{s=1}^S \frac{1}{2^t} \sum_{k=1}^{2^t} |f_{\mathbf{Y}^{(s)}}^{\text{KDE}}(\mathbf{p}_k^l) - f(\mathbf{p}_k^l)|^2,
\end{aligned}$$

where $l > 0$ is a truncation parameter, $\mathbf{Y}^{(1)}, \dots, \mathbf{Y}^{(S)}$ are Monte Carlo replications of the sample set and

$$\mathbf{p}_k^l = 2l\mathbf{w}_k - l\mathbf{1} \in [-l, l]^d, \quad k = 1, 2, \dots, 2^t,$$

with $\{\mathbf{w}_k\}_{k=1}^{2^t}$ being the first 2^t points of the d -dimensional Sobol' sequence, which is mentioned in [10].

For the PSKK estimator $f_{\mathbf{Y}}^\lambda$, we decompose the MISE as

$$\begin{aligned}
\text{MISE}(f_{\mathbf{Y}}^\lambda) &:= \mathbb{E} \left[\int_{\mathbb{R}^d} |f_{\mathbf{Y}}^\lambda(\mathbf{x}) - f(\mathbf{x})|^2 d\mathbf{x} \right] \\
&= \mathbb{E} \left[\int_{[-a,a]^d} |f_{\mathbf{Y}}^\lambda(\mathbf{x}) - f(\mathbf{x})|^2 d\mathbf{x} \right] + \int_{\mathbb{R}^d \setminus [-a,a]^d} f(\mathbf{x})^2 d\mathbf{x}.
\end{aligned}$$

The first term on the right hand side is estimated via

$$\text{(F.2)} \quad \mathbb{E} \left[\int_{[-a,a]^d} |f_{\mathbf{Y}}^\lambda(\mathbf{x}) - f(\mathbf{x})|^2 d\mathbf{x} \right] \approx \frac{(2a)^d}{S} \sum_{s=1}^S \frac{1}{2^t} \sum_{k=1}^{2^t} |f_{\mathbf{Y}^{(s)}}^\lambda(\mathbf{p}_k^a) - f(\mathbf{p}_k^a)|^2,$$

where $\mathbf{Y}^{(s)}$ for $s = 1, \dots, S$ and \mathbf{p}_k^a for $k = 1, \dots, 2^t$ follow the same definitions as in (F.1). For the second term, we compute it using 10^8 Monte Carlo samples drawn from $f(\mathbf{x})$.

In our numerical experiments, we set $l = 6, t = 16$ and $S = 20$. The truncation parameter l for the MISE of KDE ensures that the MISE truncation error is at least one order of magnitude smaller than the estimated MISE of KDE, while S guarantees that the Monte Carlo confidence interval width is at least ten times smaller than the MISE value.

Appendix G. Supplement to Example 2: Impact of parameters a, N , and λ on MISE. This section extends the 4-dimensional Gaussian mixture density estimation study from Example 2 (Subsection 6.2). Using the same target density, we systematically examine how parameters α, a, N , and λ influence the MISE of the PSKK estimator.

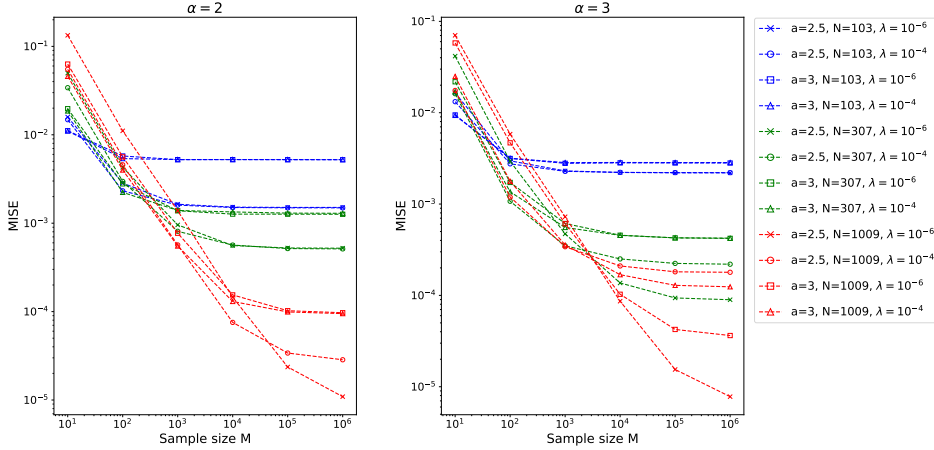


FIG. G.1. Plot of MISE convergence of the PSKK method for $N = 103, 307, 1009, a = 2.5, 3$, and $\lambda = 10^{-4}, 10^{-6}$, with $\alpha = 2$ (left), 3 (right).

Figure G.1 shows the decay of MISE of the PSKK method for $N = 103, 307, 1009$, with $a = 2.5, 3$ and $\lambda = 10^{-4}, 10^{-6}$. In the left panel, we set $\alpha = 2$, while in the right panel $\alpha = 3$ is used. It is evident that, with a sufficiently large sample size M , the MISE of the PSKK method diminishes as N increases. However, we report that increasing N beyond $N = 1009$ did not help decrease the error. We interpret this as the term involving N in the MISE bound (4.9) being negligible when N exceeds 1009 under the current sample size.

Next, we analyze the behavior of the MISE for varying values of a while keeping N fixed. Figure G.2 illustrates the MISE decay of the PSKK method for $N = 1009$ and different parameter combinations: $a = 1.5, 2, 2.5, 3, \lambda = 10^{-4}, 10^{-5}, 10^{-6}$ and $\alpha = 2, 3$. It can be observed that in the 4-dimensional example, the MISE is highly sensitive to the parameter a . Excessively large or small values of a can result in an increased MISE. Specifically, smaller values of a lead to a significant difference between f and \hat{f} , and the support of the estimator becomes relatively small, thereby increasing truncation errors. Conversely, larger values of a increase the projection

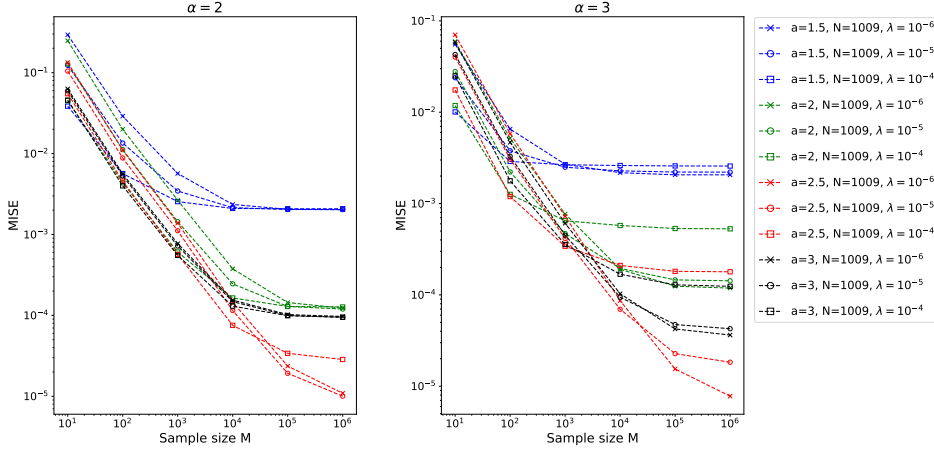


FIG. G.2. Plot of MISE convergence of the PSKK method for $N = 1009$, $a = 1.5, 2, 2.5, 3$, and $\lambda = 10^{-4}, 10^{-5}, 10^{-6}$, with $\alpha = 2$ (left), 3 (right).

error and variance bound. For this particular example, when dealing with larger sample sizes, a recommended value for a is approximately 2.5.

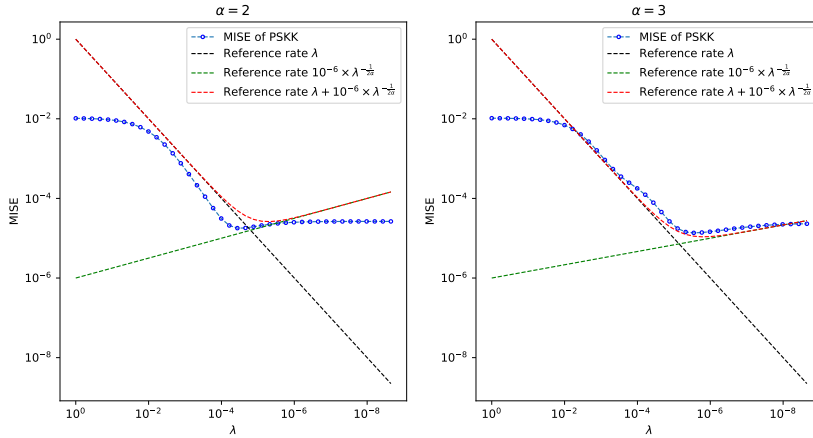


FIG. G.3. Plot of MISE for $\alpha = 2$ (left), 3 (right), $N = 1009$, $a = 2.5$, and $M = 10^5$ with $\lambda = 0.6^k$, $k = 0, 1, \dots, 39$.

In Figure G.3, we fix $a = 2.5$, $N = 1009$, $M = 10^5$ and analyze the relationship between MISE and λ . For $\alpha = 2$ and $\alpha = 3$, we compute the MISE of the PSKK method for $\lambda = 0.6^k$, where $k = 0, 1, \dots, 39$. In the case of $\alpha = 3$ (see the right panel of Figure G.3), from $\lambda = 0.6^8 \approx 0.017$ to $\lambda = 0.6^{25} \approx 2.8 \times 10^{-6}$, we see the MISE decays almost linearly in λ . Then, from $\lambda = 0.6^{25} \approx 2.8 \times 10^{-6}$ to $\lambda = 0.6^{39} \approx 2.2 \times 10^{-9}$, the MISE increases at a rate of $10^{-6} \lambda^{-\frac{1}{2\alpha}} = 10^{-6} \lambda^{-\frac{1}{6}}$. The MISE is approximately controlled by $\lambda + 10^{-6} \lambda^{-\frac{1}{2\alpha}}$. For the case where $\alpha = 2$ (see the left panel of Figure G.3), we observed similar results. These findings agree with the relationship between the

MISE bound and λ as outlined in (4.9). Furthermore, we observe that for sufficiently small λ , the MISE increases slowly as λ decreases. Therefore, selecting a λ smaller than the inflection point is acceptable in practice.

Appendix H. Higher dimensional examples. In this section, we consider higher dimensional Gaussian mixture distributions. We compare the MISE between the PSKK method and the KDE method using a density function similar to that in Subsection 6.2, but with the component means $\boldsymbol{\mu}_k$ adapted to the d -dimensional space. Specifically, the modified means are:

$$\begin{aligned}\boldsymbol{\mu}_k^{(4)} &= \left(\left\{ \frac{k}{9} \right\} - \frac{4}{9}, \left\{ \frac{2k}{9} \right\} - \frac{4}{9}, \left\{ \frac{4k}{9} \right\} - \frac{4}{9}, \left\{ \frac{8k}{9} \right\} - \frac{4}{9} \right)^\top, \\ \boldsymbol{\mu}_k^{(5)} &= \left(\left\{ \frac{k}{9} \right\} - \frac{4}{9}, \left\{ \frac{2k}{9} \right\} - \frac{4}{9}, \left\{ \frac{4k}{9} \right\} - \frac{4}{9}, \left\{ \frac{6k}{9} \right\} - \frac{4}{9}, \left\{ \frac{8k}{9} \right\} - \frac{4}{9} \right)^\top, \\ \boldsymbol{\mu}_k^{(6)} &= \left(\left\{ \frac{k}{9} \right\} - \frac{4}{9}, \left\{ \frac{2k}{9} \right\} - \frac{4}{9}, \left\{ \frac{4k}{9} \right\} - \frac{4}{9}, \left\{ \frac{6k}{9} \right\} - \frac{4}{9}, \left\{ \frac{7k}{9} \right\} - \frac{4}{9}, \left\{ \frac{8k}{9} \right\} - \frac{4}{9} \right)^\top.\end{aligned}$$

TABLE H.1
MISE of PSKK and KDE

M	$d = 4$		$d = 5$		$d = 6$	
	PSKK	KDE	PSKK	KDE	PSKK	KDE
10^1	1.75×10^{-1}	1.20×10^{-2}	8.74×10^{-2}	5.99×10^{-3}	1.98×10^{-2}	1.83×10^{-3}
10^2	1.59×10^{-2}	1.89×10^{-3}	7.62×10^{-3}	8.57×10^{-4}	2.05×10^{-3}	3.68×10^{-4}
10^3	1.53×10^{-3}	6.11×10^{-4}	8.08×10^{-4}	3.37×10^{-4}	2.02×10^{-4}	1.72×10^{-4}
10^4	1.57×10^{-4}	2.30×10^{-4}	1.02×10^{-4}	1.44×10^{-4}	4.05×10^{-5}	7.88×10^{-5}
10^5	1.94×10^{-5}	7.49×10^{-5}	3.39×10^{-5}	5.34×10^{-5}	2.29×10^{-5}	3.43×10^{-5}
10^6	5.77×10^{-6}	2.48×10^{-5}	2.70×10^{-5}	2.01×10^{-5}	2.09×10^{-5}	1.44×10^{-5}

Table H.1 presents the MISE for both the PSKK method and the KDE method in dimensions 4, 5 and 6. For the PSKK method, we set $N = 1009$, $\lambda = 10^{-6}$ and $\alpha = 2$, with truncation $a = 2.5$ for the 4-dimensional case and $a = 2$ for higher dimensions. Figures G.1 and G.2 demonstrate that the MISE of the PSKK method initially follows the theoretical convergence rate until reaching a “turning point”, after which it stabilizes. This “turning point” depends on parameters including N , a and d . As shown in Table H.1, “turning point” occurs earlier with increasing dimensionality. Furthermore, it should be mentioned that the convergence rate of the PSKK method will not change before reaching the “turning point” even for higher dimensions. Compared with the KDE method, the PSKK method has advantages in theoretical convergence rate, although achieving these rates requires more careful parameter selection than the simple fixed parameters used here.

REFERENCES

- [1] C. AGOSTINELLI, *Robust estimation for circular data*, Computational Statistics & Data Analysis, 51 (2007), pp. 5867–5875.
- [2] J. ALQUICIRA-HERNANDEZ AND J. E. POWELL, *Nebulosa recovers single-cell gene expression signals by kernel density estimation*, Bioinformatics, 37 (2021), pp. 2485–2487.

- [3] E. AMRANI, R. BEN-ARI, D. ROTMAN, AND A. BRONSTEIN, *Noise estimation using density estimation for self-supervised multimodal learning*, in Proceedings of the AAAI Conference on Artificial Intelligence, vol. 35, 2021, pp. 6644–6652.
- [4] T. BOS AND J. SCHMIDT-HIEBER, *A supervised deep learning method for nonparametric density estimation*, Electronic Journal of Statistics, 18 (2024), pp. 5601–5658.
- [5] D. W. BOYD AND J. M. STEELE, *Lower bounds for nonparametric density estimation rates*, The Annals of Statistics, 6 (1978), pp. 932–934.
- [6] Y.-C. CHEN, *A tutorial on kernel density estimation and recent advances*, Biostatistics & Epidemiology, 1 (2017), pp. 161–187.
- [7] R. COOLS, F. KUO, D. NUYENS, AND I. SLOAN, *Fast component-by-component construction of lattice algorithms for multivariate approximation with POD and SPOD weights*, Mathematics of Computation, 90 (2021), pp. 787–812.
- [8] R. COOLS, F. KUO, D. NUYENS, AND I. H. SLOAN, *Lattice algorithms for multivariate approximation in periodic spaces with general weight parameters*, vol. 754 of Contemp. Math., American Mathematical Society, 2020, pp. 93–113.
- [9] M. DI MARZIO, A. PANZERA, AND C. C. TAYLOR, *Kernel density estimation on the torus*, Journal of Statistical Planning and Inference, 141 (2011), pp. 2156–2173.
- [10] J. DICK, F. Y. KUO, AND I. H. SLOAN, *High-dimensional integration: the quasi-Monte Carlo way*, Acta Numerica, 22 (2013), pp. 133–288.
- [11] A. DITKOWSKI, G. FIBICH, AND A. SAGIV, *Density estimation in uncertainty propagation problems using a surrogate model*, SIAM/ASA Journal on Uncertainty Quantification, 8 (2020), pp. 261–300.
- [12] P. DUHAMEL AND M. VETTERLI, *Fast fourier transforms: a tutorial review and a state of the art*, Signal processing, 19 (1990), pp. 259–299.
- [13] M. D'ERRICO, E. FACCO, A. LAIO, AND A. RODRIGUEZ, *Automatic topography of high-dimensional data sets by non-parametric density peak clustering*, Information Sciences, 560 (2021), pp. 476–492.
- [14] M. GRIEBEL AND M. HEGLAND, *A finite element method for density estimation with Gaussian process priors*, SIAM Journal on Numerical Analysis, 47 (2010), pp. 4759–4792.
- [15] A. HALLIN, J. ISAACSON, G. KASIECZKA, C. KRAUSE, B. NACHMAN, T. QUADFASSEL, M. SCHLAFFER, D. SHIH, AND M. SOMMERHALDER, *Classifying anomalies through outer density estimation*, Physical Review D, 106 (2022), p. 055006.
- [16] M. HEGLAND, G. HOOKER, AND S. ROBERTS, *Finite element thin plate splines in density estimation*, The Proceedings of ANZIAM, 42 (2000), pp. C712–C734.
- [17] V. KAARNIOJA, Y. KAZASHI, F. Y. KUO, F. NOBILE, AND I. H. SLOAN, *Fast approximation by periodic kernel-based lattice-point interpolation with application in uncertainty quantification*, Numerische Mathematik, (2022), pp. 1–45.
- [18] T. KANAMORI, S. HIDO, AND M. SUGIYAMA, *A least-squares approach to direct importance estimation*, The Journal of Machine Learning Research, 10 (2009), pp. 1391–1445.
- [19] T. KANAMORI, T. SUZUKI, AND M. SUGIYAMA, *Statistical analysis of kernel-based least-squares density-ratio estimation*, Machine Learning, 86 (2012), pp. 335–367.
- [20] Y. KAZASHI AND F. NOBILE, *Density estimation in RKHS with application to Korobov spaces in high dimensions*, SIAM Journal on Numerical Analysis, 61 (2023), pp. 1080–1102.
- [21] N. M. KOROBV, *Number-Theoretic Methods in Approximate Analysis*, Fizmatgiz, Moscow, 1963.
- [22] D. P. LAURIE, *Periodizing transformations for numerical integration*, Journal of computational and applied mathematics, 66 (1996), pp. 337–344.
- [23] Q. LIU, J. XU, R. JIANG, AND W. H. WONG, *Density estimation using deep generative neural networks*, Proceedings of the National Academy of Sciences, 118 (2021), p. e2101344118.
- [24] S. McDONALD AND D. CAMPBELL, *A review of uncertainty quantification for density estimation*, Statistics Surveys, 15 (2021), pp. 1–71.
- [25] R. NASRI, J. JAMII, M. MANSOURI, Z. AFFI, AND V. PUIG, *A novel data-driven MPC framework using KDE and KPCA for autonomous vehicles*, IEEE Access, (2025).
- [26] A. NODEHI, M. GOLALIZADEH, M. MAADOOLIAT, AND C. AGOSTINELLI, *Estimation of parameters in multivariate wrapped models for data on a p-torus*, Computational Statistics, 36 (2021), pp. 193–215.
- [27] D. NUYENS AND Y. SUZUKI, *Scaled lattice rules for integration on \mathbb{R}^d achieving higher-order convergence with error analysis in terms of orthogonal projections onto periodic spaces*, Mathematics of Computation, 92 (2023), pp. 307–347.
- [28] F. W. J. OLVER, A. B. O. DAALHUIS, D. W. LOZIER, B. I. SCHNEIDER, R. F. BOISVERT, C. W. CLARK, B. R. MILLER, B. V. SAUNDERS, H. S. COHL, AND M. A. E. MCCLAIN, *NIST digital library of mathematical functions*. <http://dlmf.nist.gov/>.

- [29] B. PEHERSTORFER, D. PFLÜGE, AND H.-J. BUNGARTZ, *Density estimation with adaptive sparse grids for large data sets*, in Proceedings of the 2014 SIAM international conference on data mining, SIAM, 2014, pp. 443–451.
- [30] L. K. RAJENDRAN, J. ZHANG, S. BHATTACHARYA, S. P. BANE, AND P. P. VLACHOS, *Uncertainty quantification in density estimation from background-oriented Schlieren measurements*, Measurement Science and Technology, 31 (2020), p. 054002.
- [31] A. RAY, *Emulating compact binary population synthesis simulations with robust uncertainty quantification and model comparison: Bayesian normalizing flows*, arXiv preprint arXiv:2506.05657, (2025).
- [32] S. G. ROBERTS AND S. BOLT, *A note on the convergence analysis of a sparse grid multivariate probability density estimator*, The Proceedings of ANZIAM, 50 (2008), pp. C858–C870.
- [33] A. SIDI, *A new variable transformation for numerical integration*, in Numerical Integration IV: Proceedings of the Conference at the Mathematical Research Institute, Oberwolfach, November 8–14, 1992, Springer, 1993, pp. 359–373.
- [34] B. W. SILVERMAN, *Density estimation for statistics and data analysis*, Routledge, New York, 2018.
- [35] B. SRIPERUMBUDUR, K. FUKUMIZU, A. GRETTON, A. HYVÄRINEN, AND R. KUMAR, *Density estimation in infinite dimensional exponential families*, Journal of Machine Learning Research, 18 (2017), pp. 1–59.
- [36] M. STEININGER, K. KOBIS, P. DAVIDSON, A. KRAUSE, AND A. HOTH, *Density-based weighting for imbalanced regression*, Machine Learning, 110 (2021), pp. 2187–2211.
- [37] M. SUGIYAMA, T. SUZUKI, AND T. KANAMORI, *Density-ratio matching under the Bregman divergence: a unified framework of density-ratio estimation*, Annals of the Institute of Statistical Mathematics, 64 (2012), pp. 1009–1044.
- [38] M. K. VARANASI AND B. AAZHANG, *Parametric generalized Gaussian density estimation*, The Journal of the Acoustical Society of America, 86 (1989), pp. 1404–1415.
- [39] Z. WANG AND D. W. SCOTT, *Nonparametric density estimation for high-dimensional data—Algorithms and applications*, Wiley Interdisciplinary Reviews: Computational Statistics, 11 (2019), p. e1461.
- [40] M. WONG AND M. HEGLAND, *Maximum a posteriori density estimation and the sparse grid combination technique*, The Proceedings of ANZIAM, 54 (2012), pp. C508–C522.
- [41] A. ZANDIEH, I. HAN, M. DALIRI, AND A. KARBASI, *Kdeformer: Accelerating transformers via kernel density estimation*, in International Conference on Machine Learning, PMLR, 2023, pp. 40605–40623.
- [42] W. ZELLINGER, S. KINDERMANN, AND S. V. PEREVERZYEV, *Adaptive learning of density ratios in RKHS*, Journal of Machine Learning Research, 24 (2023), pp. 1–28.